



PROMOVENDI

The Book of Articles

National Scientific Conference

“Understand the Science”

V edition,

September 25, 2021

National Scientific Conference

“e-Factory of Science”

VI edition,

November 20, 2021



www.promovendi.pl



[fundacja.promovendi](https://www.facebook.com/fundacja.promovendi)

Organizer:

Promovendi Foundation

Chairman of the Organizing Committee:

Firaza Agnieszka

Members of the Organizing Committee:

Byczkowska Paulina

Graczyk Andrzej

Perek-Długosz Aleksandra

Solarczyk Paweł

Editor:

Kępczak Norbert

Solarczyk Paweł

Promovendi Foundation Publishing

Address:

17/19/28 Kamińskiego st.

90-229 Łódź, Poland

KRS: 0000628361

NIP: 7252139787

REGON: 364954217

e-mail: fundacja@promovendi.pl

www.promovendi.pl

ISBN: 978-83-961157-8-2

The papers included in this Book of Articles have been printed in accordance with the submitted texts after they have been accepted by the reviewers. The authors of individual papers are responsible for the lawful use of the materials used.

Open Access

November, 2021

Scientific Committee:

Assoc. Prof. D.Sc. Ph.D. Andrzej Szosland – Lodz University of Technology
Assoc. Prof. D.Sc. Ph.D. Marta Kadela – Building Research Institute in Warsaw
Assoc. Prof. D.Sc. Ph.D. Jacek Sawicki – Lodz University of Technology
Assoc. Prof. D.Sc. Ph.D. Kamila Puppel – Warsaw University of Life Sciences – SGGW
D.Sc. Ph.D. Ryszard Wójcik – The Jacob of Paradies University in Gorzów Wielkopolski
Ph.D. Norbert Kępczak – Lodz University of Technology
Ph.D. Przemysław Kubiak – Lodz University of Technology
Ph.D. Monika Kulisz – Lublin University of Technology
Ph.D. Rafał Miśko – Wrocław University of Science and Technology
Ph.D. Łukasz Jan Niewiara – Nicolaus Copernicus University in Toruń
Ph.D. Aleksandra Perek-Długosz – Technologie Galwaniczne Sp. z o.o.
Ph.D. Martyna Rabenda – Skanska S.A.
Ph.D. Radosław Rosik – Lodz University of Technology
Ph.D. Olga Shtyka – Lodz University of Technology
Ph.D. Piotr Synowiec – Wrocław University of Science and Technology
Ph.D. Joanna Szala-Bilnik – University of Alabama, US
Ph.D. Robert Święcik – Lodz University of Technology

Reviewers:

Prof. D.Sc. Ph.D. Kazimierz Baczewski – Military University of Technology in Warsaw
Assoc. Prof. D.Sc. Ph.D. Radomir Jasiński – Cracow University of Technology
Assoc. Prof. D.Sc. Ph.D. Grzegorz Krzykowski – WSB University in Gdańsk
Assoc. Prof. D.Sc. Ph.D. Piotr Świercz – Jesuit University Ignatianum in Krakow
Assoc. Prof. D.Sc. Ph.D. Monika Wilamowska-Zawłocka – Gdańsk University of Technology
Ph.D. Norbert Olczyk – West Pomorian University of Technology in Szczecin

TABLE OF CONTENTS

Barczak Beata, Kazimierski Pawel, Łuczak Justyna, Klugmann-Radziemska Ewa, Januszewicz Katarzyna <i>Activated biochar as an adsorbent of organic pollutants for water and wastewater treatment.....</i>	5
Filipiuk Tomasz <i>Devices for monitoring the technical condition of engine oils.....</i>	16
Gierszewska Natalia, Uciurkiewicz Jakub, Blyszko Jarosław <i>3D printing with mixes with high-alumina cements – state of art.....</i>	24
Kawiak Natalia <i>The perception of sexual minorities in poland in surveys.....</i>	29
Kępys Andrzej, Syska Ernest <i>Veo weather routing – an innovative algorithm for calculating routes based on weather, map and polar plots of yachts.....</i>	36
Uciurkiewicz Jakub, Gierszewska Natalia, Blyszko Jarosław <i>Cement mixtures for 3D printing with high alumina cement as setting time regulator – experimental approach.....</i>	49
Zawadzińska Karolina, Kula Karolina <i>Application of the molecular electron density theory to describe the reactivity of nitrile N-oxides and selectivity of their reactions with selected π-deficient unsaturated components..</i>	57

ACTIVATED BIOCHAR AS AN ADSORBENT OF ORGANIC POLLUTANTS FOR WATER AND WASTEWATER TREATMENT

Beata Barczak¹, Pawel Kazimierski², Justyna Łuczak³, Ewa Klugmann-Radziemska¹,
Katarzyna Januszewicz^{1*}

¹ Department of Energy Conversion and Storage, Faculty of Chemistry, Gdansk University of Technology, Gdansk

²Renewable Energy Department, Institute of Fluid-flow Machinery PAN, Gdansk

³Department of Process Engineering and Chemical Technology, Faculty of Chemistry, Gdansk University of Technology, Gdansk

* corresponding author: katarzyna.januszewicz@pg.edu.pl

Abstract:

Biomass, especially waste biomass, as an alternative energy source is today's significant issue. Pyrolysis is a process of thermal degradation of raw material, and one of its products is biochar. This product is characterised by high carbon content, and improving its quality through activation allows for its wider use. Chemical activation improves the quality of carbon materials by applying high temperatures and an activator, e.g. KOH. This method allows obtaining sorption materials with a highly developed specific surface area of more than 1100 m²/g. Pyrolysis of waste biomass, which consisted of corn cobs and cherry stones, was performed. The results of the study of the adsorption capacity of organic pollutants from the aqueous phase by the activated biocarbon are presented. An aqueous solution of Rhodamine B was used as a model pollutant. The study discusses the effect of waste biomass type on organic pollutants' adsorption capacity.

Keywords:

pyrolysis, chemical activation, waste biomass, activated biocarbon, adsorption

Introduction

Waste biomass includes solid or liquid biodegradable substances of animal or plant origin, which come from the food industry, agriculture, forestry production, and processing industry [1, 2]. It consists mainly of carbohydrate polymers such as cellulose, hemicellulose, and lignin [3]. The proportions of the individual components depend on the origin of the biomass and influence its properties, and the non-nutritive part can be used in further processing [4]. A distinction is made between hard and soft biomass [5]. Soft biomass, such as chestnut wood, linden wood or willow wood, contain less lignin than hard biomass (e.g. fruit stones or oak wood) [6-9].

Waste biomass, one of the most popular sources of renewable energy, is used in thermal conversion to valuable products. The thermal conversion of chemical energy from biomass can be accomplished by combustion (direct process) or gasification/pyrolysis, during which one form of fuel is transformed into another (indirect processes) [10].

Pyrolysis is the process of degradation of a complex molecule of a chemical compound occurring in an anaerobic atmosphere under a high temperature. Three products, namely, solid (char), liquid (oil) and gas fraction, are received in the process [11]. The main factors determining how the process is carried out are temperature and heating rate. Therefore, four types of pyrolysis can be distinguished: low-temperature (450-700°C) and high-temperature (900-1200°C), fast and slow [12].

Raw char has a low commercial value, can be directly incinerated. Nevertheless, the product can also be subjected to activation processes to improve its quality and adsorption properties [13, 14]. The different structures and properties of chars are due to differences in the feedstock material [11, 15]. The basic raw materials used to produce activated carbons include coal and lignite, wood, peat, fruit stones, and shells [1, 16-18]. Due to their sorption properties, activated biocarbon find applications in many fields such as water treatment, energy storage, catalysis and gas purification [19-21].

During activation, either chemical or physical, an oxidising agent is acted on the carbon material [9]. The first stage in both processes is usually carbonisation, while the second step involves the action of a gaseous oxidising agent (steam or carbon dioxide) on the chars at 800-1000°C [22]. This process is widely used on an industrial scale, but chemical activation is of greater interest on a laboratory scale. Chemical activation can be carried out in a one-step or two-step process. The first method involves impregnating the biomass with an activating agent (e.g. H_3PO_4 , ZnCl_2) and then subjecting the mixture to high temperature. At the same time, the second requires prior carbonisation of the biomass, followed by impregnation with an activator (KOH , NaOH , and K_2CO_3) and annealing of the mixture at high temperature [23-25]. The chemical activation of chars with alkaline substances produces alkali metals and carbonates, which improve the stability of the carbon matrix and expand the space between carbon-atom layers, thus increasing the efficiency and adsorption capacity of the resulting activated carbon [25]. Another factor affecting the properties of sorption materials is the ratio of activator to carbon precursor. Generally, increasing the activator ratio results in the development of a microporous structure at the expense of the mesoporous structure. In conclusion, chemical activation is a better method than physical activation, even though it requires more work due to eliminating activator residues. Nevertheless, it produces microporous materials with a higher specific surface area [26, 27].

Despite significant progress in the preparation and characterisation of carbon materials, a method to obtain products with high structural parameters from low-cost raw materials, such as waste biomass, is still being sought [8]. In this regard, this work presents a high-efficiency method to obtain active biochar from corn cobs and cherry stones by chemical activation with potassium hydroxide. The choice of raw materials was dictated primarily by Poland's largest producer of cherries in the European Union. These fruits are used in the processing industry in more than 70% [28]. Corn cobs, in turn, are an agricultural waste and an example of soft biomass with a high calorific value and low nitrogen and sulfur content [29, 30]. Therefore, the obtained biocarbon were chemically activated, their structure was characterised, and their ability to adsorb organic model pollutants from the aqueous phase was evaluated.

Materials and methods

Two types of waste biomass were chosen as substrates for pyrolysis: cherry stones and corn cobs. The corn cobs were ground into the homogenous material in a size of 0.3-0.5 cm. Raw materials were pyrolysed in a muffle furnace type BEM in stainless steel reactor. The volatile fraction was generated during the pyrolysis process, transported in the pipe and collected in the steel tank after cooling with the water cooler. The process was carried out in both cases at 800°C in an oxygen-free atmosphere, without flow gas.

Chemical activation

Before the activation process, the solid fraction from the pyrolysis- char was ground in a mortar to a particle size of about 1 mm, in both cases. The 5 g of the char was weighed and mixed with an equivalent amount of KOH (1:1) in the case of corn cobs, while twice the mass excess of activator (2:1) was used for cherry kernels. Then, 30 mL of distilled water was added and stirred for 2 h at 50°C. The efficiency of influencing the ratio of activator on the high surface area of char was conducted previously for both samples [31]. The samples were dried overnight at 105°C. The raw materials in porcelain crucibles were placed in quartz tubes in a horizontal cylindrical furnace at 900°C for 2 h under an atmosphere of nitrogen as an inert gas. After the activation process, Hielscher ultrasonic homogeniser was used for 3 minutes twice to remove residual KOH. The water excess (200 mL) was added for dilution of activator and to the solid fraction sediment during 48 h. The liquid alkali solution was decanted and neutralised with the solution of hydrochloric acid. The suspension was filtrated under vacuum using a Büchner funnel (0.3 mm thick, 0.7 µm particle size retained). The solid residue was washed with water to neutralisation the filtrate. The activated carbons were dried overnight at 80°C and further analysed.

Characteristics of activated biocarbon

The obtained activated carbons were subjected to nitrogen adsorption analysis, according to the Brunauer, Emmett and Teller (BET) model of multilayer adsorption isotherms, to determine their specific surface area (S_{BET}) and pore volume (V_P). Samples were degassed 2 h prior to measurement. Before the measurement, the degassed samples were weighed and then analysed using a BET specific surface area analyser (Micrometrics Gemini V). The parameters are determined to allow the pore diameter (D_p) to be determined using the following formula [32].

$$D_p = \frac{4V_P}{S_{BET}} \quad (1)$$

where:

V_P – pore volume [m^3/g];

S_{BET} – surface area [m^2/g];

D_p – pore diameter [m].

Fourier transform infrared spectroscopic (FT-IR) analysis was performed to determine the effect of the chemical activation process on the formation of surface functional groups. First, the 0.55-1 mg of the obtained activated carbons were weighed, then potassium bromide was added, and a tablet was

made from the mixture using a hydraulic press. Finally, the obtained tablet was analysed, and the spectrum was recorded (Nicolet iS10).

The morphology of the samples was analysed using scanning electron microscopy (SEM) (Hitachi SU3500).

Adsorption studies

In order to study the adsorption capacity of organic pollutants from the aqueous phase, the model organic compound Rhodamine B was used. A stock solution of the Rhodamine B (1000 mg/L) was prepared in deionised water was diluted to a concentration of 10-100 mg/L to prepare a series of standard solutions for the calibration curve. In order to determine the rate of RhB adsorption, the experiments were conducted with different amounts of adsorbent at a constant initial concentration of Rhodamine B, temperature, pH and particle size. The activated carbon (AC) was added at different doses in the range from 2.5-150 mg into 10 mL RhB solution (30 mg/L [33]). The samples were mixed and left overnight. The samples were then filtered at the same time intervals, and the concentrations of dye solutions were analysed by UV-VIS spectrophotometer at 553 nm (UV-VIS Evolution 220, Thermo Scientific).

Results and discussion

Structure characteristics of activated carbons

During the experimental engineering study, the KOH : char mass ratio was optimised, based on which the most effective activation ratios for both biomass samples were selected [31]. In this work, the samples with the highest specific surface area(SSA) are presented. The analyses of the specific surfaces of the obtained activated biocarbon indicate the effectiveness of the chosen method of chemical activation with KOH. As a result of the activation process, two activated carbons AC_{corn cob} and AC_{cherrystone} were obtained. The carbon material AC_{corn cob} had a specific surface area of 1143.2 m²/g, while AC_{cherrystone} had a specific surface area of 1116.2 m²/g. These values indicate a highly developed surface morphology of the obtained activated carbons. According to literature data, the char of corn cobs has a SSA of about 8 m²/g, and the char of cherry stones has a SSA of 80 m²/g, which indicates the high efficiency of the chemical activation process carried out [34, 35].

Tab. 1. Surface area (S_{BET}), pore size (V_P) and pore density (D_p) of the activated carbons obtained from the corn cob and cherry stones

	KOH:AC (mass ratio)	S_{BET} [m ² /g]	V_P [cm ³ /g]	D_p [nm]
AC _{corn cob}	1:1	1143.2	0.57	1.99
AC _{cherrystone}	2:1	1116.2	0.56	2.01

Source: [31]

The results presented in Table 1 confirm the highly developed specific surface area and porous structure (Tab. 1). The pore diameter belonging to the micropore range (2 nm) indicates high penetration of the carbon material by activator KOH and indicate the potentially high sorption capacity of the obtained carbon materials. The *F.O. Erdogan*, during the chemical activation of cherry seeds with KOH, obtained activated carbons with a specific surface area of 1380 m²/g [36].

The difference in specific surface areas compared to the literature value may be due to the longer impregnation time of the biochar, as well as the use of the ultrasonic activation technique at 200-300°C in the mentioned studies [36].

The morphology of activated carbon samples was analysed by scanning electron microscopy (SEM), and the results are shown in Fig. 1. The structure of the chars before activation was more irregular, jagged and uneven. Residues of the inorganic fraction are also observed (as white marks). In contrast, after the activation process, the structure became more uniform and ordered. Furthermore, it was observed that as the specific surface area increased, the number of individual particles decreased, and the structure became less jagged. The activation process results in the formation and enlargement of pores, but the original spatial skeleton is retained. In the case of corn cob biomass products, the characteristic structure of hexagons with holes is observed. Similar observations were made in the work of J. Kaźmierczak [37].

Moreover, activation results in the reduction of inorganic residues after the pyrolysis of biomass. The micrographs obtained confirm that chemical activation by KOH favours the formation of a well-developed microporous structure inside the raw material, which is responsible for the corresponding specific surface area. SEM images confirm significant between the chars obtained by pyrolysis of corn cobs and cherry stoned and the products obtained by their chemical activations. However, the materials differ significantly in the arrangement, number and size of pores.

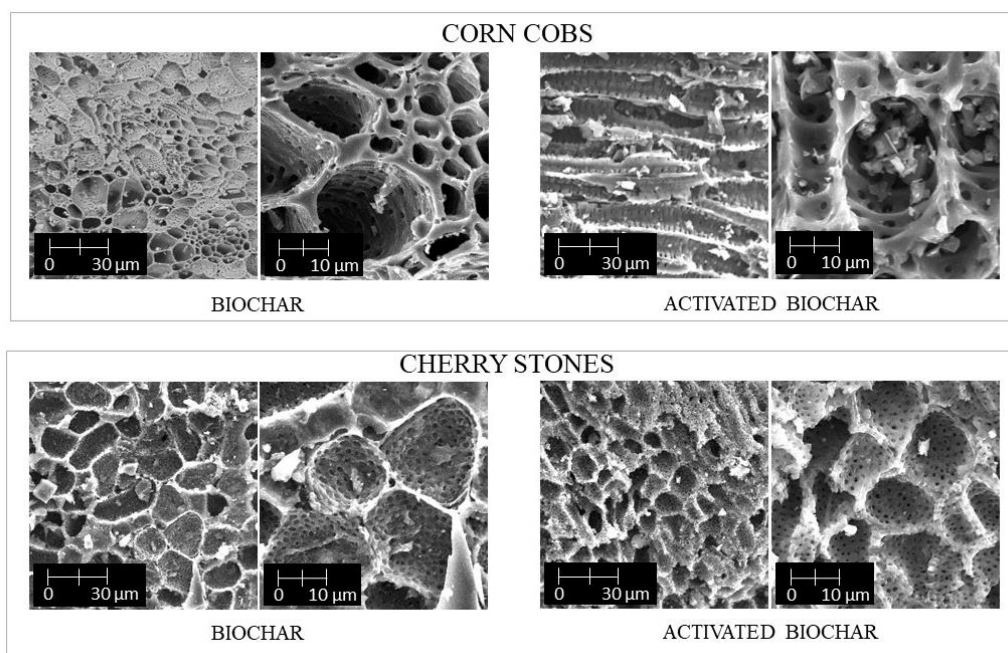


Fig. 1. Comparison of corn cob and cherry seed samples before and after chemical activation: SEM micrographs
Source: [31]

Chemical activation of both corn cob and cherry stones char samples resulted in enrichment of the structures with oxygen groups such as hydroxyl, carbonyl and ester. In addition, in the case of the AC from the fruit studied, a vibration characteristic of the cyanide group was observed. Due to the presence of cyanoglycosides in the cherry stones, hydrogen cyanide can be released during the pyrolysis process. The concentration of this substance reaches 4.6 mg/kg of fruit [38].

The characteristic vibrations occurring in the given wave numbers are shown in the table below (Tab. 2).

Tab. 2. Description of the characteristic vibrations obtained for the activated carbons and char studied

Wave number [cm^{-1}]	Description
3500 – 3300	O-H stretching vibrations, characteristic of hydroxyl groups in alcohols and phenols
3300 – 2700	O-H stretching vibrations, characteristic of a carboxyl group
2400 – 2350	C-N stretching vibrations, characteristic of the cyanide group
1670 – 1630	C=O stretching vibrations, characteristic of carbonyl and ester groups
1150 – 1080	C-O stretching vibrations, characteristic of 1st and 2nd order alcohols and esters

Source: [31]

In the case of cherry stone char, vibrations characteristic of hydroxyl and cyanide groups of slight intensity are observed (Fig. 2a). On the other hand, the chemical activation process caused significant material enrichment in oxygen groups, which is observed on the FT-IR spectrum (Fig. 2b). This is revealed by an increase in the intensity of the bands for C-O stretching vibrations characteristic of first and second-order alcohols and esters and the band corresponding to O-H stretching vibrations characteristic of hydroxyl groups.

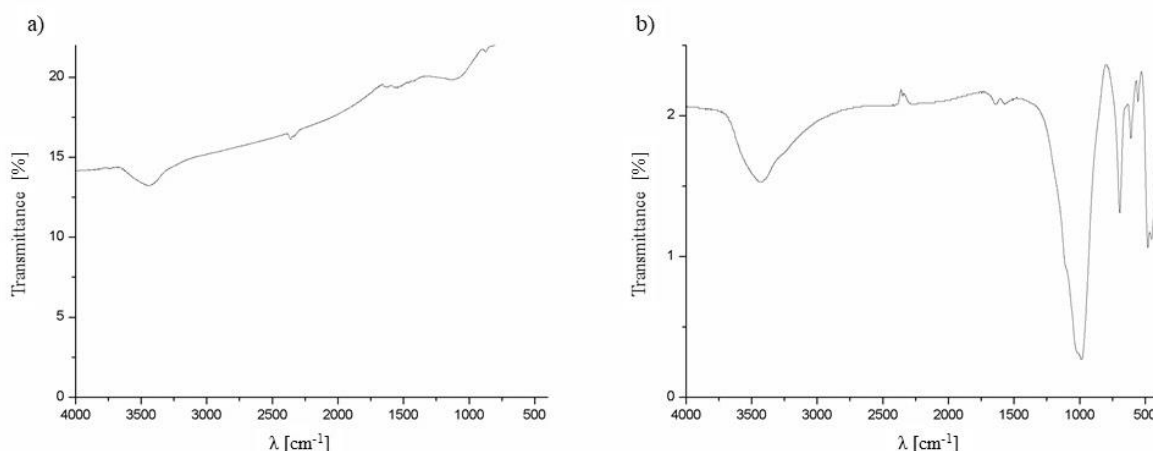


Fig. 2. FT-IR spectra of (a) cherry stone carbon black, (b) activated carbon from cherry stone biomass

Source: [31]





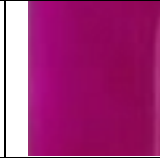





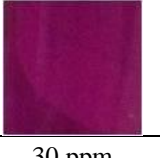
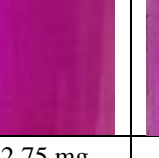
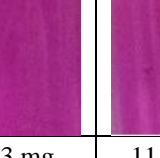

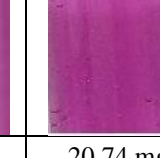
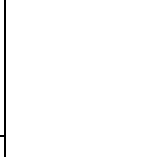
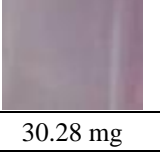
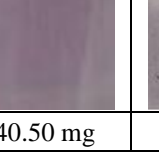
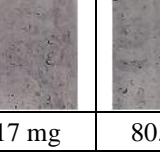
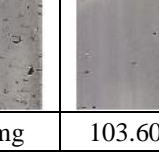
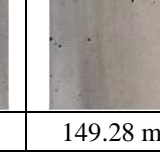
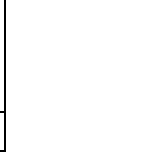
AC used as an adsorbent in wastewater treatment

The sorption properties of the carbon materials obtained were investigated using the samples with high specific surface area AC from cherry stone char ($1116.2 \text{ m}^2/\text{g}$) and corn cob char ($1143.2 \text{ m}^2/\text{g}$). Various model organic compounds were used as model organic contaminants, such as methylene blue and bromothymol blue [39,40]. In this work Rhodamine B (RhB) was chosen. A solution for the standard curve was prepared from RhB standard solution (30 ppm). Various doses of sorption materials were used:

- activated carbon from corn cobs: 2.75; 5.23; 11.02; 15.23; 20.74; 30.28; 40.50; 51.17; 80.98; 103.6 and 149.28 mg,
- activated carbon from cherry stone: 2.81; 11.27; 15.68; 30.24; 39.98; 50.90; 79.70; 98.57 and 149.88 mg.

Particle size, temperature, contact time, initial concentration, and residual ion concentration were kept constant in all dye removal experiments. The mixtures were then filtered, and the liquid was subjected to UV-VIS analysis. The colours of the resulting solutions are compared in the tables below (Tab. 3). The first picture presents the colour of the solutions without adding activated carbon (reference experiment), whereas other pictures are of samples with different addition parts of AC. In all experiments of dye removal, temperature, contact time, and initial were kept constant. Activated carbons used in different quantitative proportions resulted in the discolouration of the RhB dye solution. As expected, the adsorption efficiency increased with increasing amounts of activated carbon used in the experiment until the solution was completely discoloured. The remaining colour of the solution measured by UV-VIS spectrometry is shown in Tab. 3 and Fig. 3. Rhodamine B, as a model wastewater pollutant, is adsorbed by small amounts of activated carbon. A different degree of solution discolouration is observed depending on the mass of the sorption material (Tab. 3).

Tab. 3. Discolouration of RhB solution after application of activated carbon obtained by pyrolysis of corn cobs and cherry stones chemical activation with KOH. The photographs show the colouration of the solutions after using appropriate doses of activated biocarbon for the sorption of 30 mg/L RhB at 25°C

Activated biocarbon from cherry stones (1:1)					
					
30 ppm	2.81 mg	11.27 mg	15.68 mg	30.24 mg	
					
39.98 mg	50.90 mg	79.70 mg	98.57 mg	149.88 mg	
Activated biocarbon from corn cobs (2:1)					
					
30 ppm	2.75 mg	5.23 mg	11.02 mg	15.23 mg	20.74 mg
					
30.28 mg	40.50 mg	51.17 mg	80.98 mg	103.60 mg	149.28 mg

Source: own elaboration

As the weight of carbon increases, the concentration of Rhodamine B decreases. In the case of activated carbon from cherry stones char, complete decolourisation was observed after applying

79.70 mg of the product, whereas for corn cobs at 30.28 mg. Furthermore, the dye was wholly adsorbed for samples 1-6 and 1-3, and complete decolourisation of the solutions occurred.

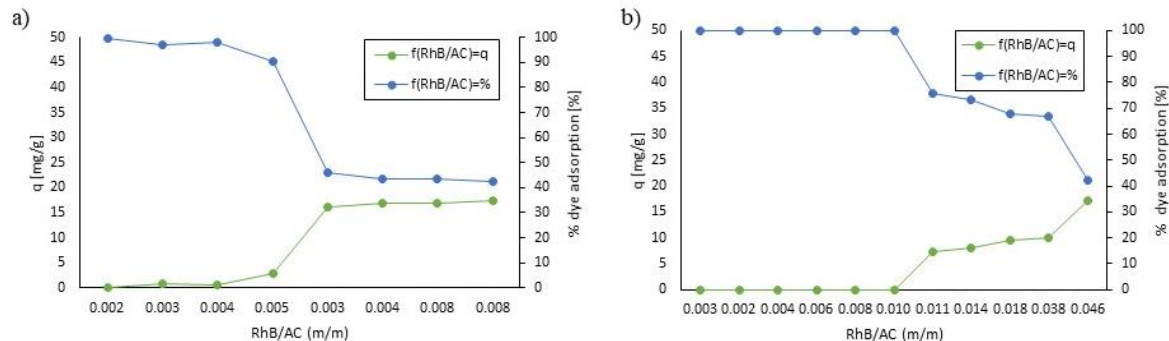


Fig. 3. Plots of the dependence of RhB concentration after adsorption and % dye removal on the RhB/AC ratio (m/m),
(a) activated carbon from cherry stones, (b) activated carbon from corn cobs

Source: [31]

Tab. 4. The adsorption parameters

No	Before adsorption			After adsorption	
	Activated carbon [mg]	Rhodamine B [mg]	RhB/AC (mass ratio)	q [mg/L]	% dye removal
W1	149.9	0.6	0.002	0.1	99.5
W2	98.6	0.6	0.003	1.0	96.8
W3	79.7	0.6	0.004	0.5	98.2
W4	50.9	0.6	0.005	2.9	90.3
W5	40.0	0.6	0.003	16.2	46.1
W6	30.2	0.6	0.004	16.9	43.7
W7	15.7	0.6	0.008	16.9	43.7
W8	11.3	0.6	0.011	17.3	42.3
W9	2.8	0.6	0.045	17.4	42.1
K1	103.6	0.6	0.003	n.d.	100.0
K2	149.3	0.6	0.002	n.d.	100.0
K3	81.0	0.6	0.004	n.d.	100.0
K4	51.2	0.6	0.006	n.d.	100.0
K5	40.5	0.6	0.008	n.d.	100.0
K6	30.3	0.6	0.010	n.d.	100.0
K7	20.7	0.6	0.011	7.2	76.0
K8	15.2	0.6	0.014	7.9	73.5
K9	11.0	0.6	0.018	9.6	68.0
K10	5.2	0.6	0.038	9.9	67.0
K11	2.7	0.6	0.046	17.3	42.5

Source: [31]

The obtained results of high surface area activated carbons confirm the potential possibility of being used as an adsorbent in wastewater treatment. Furthermore, AC from maize cob biomass has a higher sorption capacity than activated carbon from cherry kernels. AC from corn cobs has a more

developed mesoporous structure than AC from cherry kernels. The medium-sized pores are responsible for the adsorption of larger molecules, such as the Rhodamine B molecule. The sorption capacity values obtained are lower than the literature data. In the work of N. Abdolrahimi, almond shell activated carbon with an area of 1252 m²/g and pore size of 4 nm was characterised by an adsorption capacity of 255 mg/g [41]. The differences in specific surface area of samples follow from various biomass types, pyrolysis conditions, and activation methods used in compared experiments, which influence larger AC pores obtained in the present work.

Conclusion

A method for chemical activation of biocarbon, with using KOH, to improve the specific surface area and sorption properties of the material, was described. Waste biomass samples derived from agricultural (corn cobs) and food industry (cherry stones) were used for this study. Highly developed specific surface area (over 1100 m²/g) and porous structure (diameter over 2 nm) allows the use of the obtained sorbent materials as valuable products for wastewater treatment. Furthermore, activated carbon produced from maize cob had a higher sorption capacity than activated carbon from cherry kernels, as shown by water's sorption studies of the model pollutant Rhodamine B.

Activation of solid fraction from pyrolysis process may be cost-effective when considering a wide range of applications as adsorbents in methane and hydrogen storage processes, as phase change materials (PCMs), substrates for plant cultivation (fertiliser carrier) and electrode materials [42].

Literature

- [1] Z. Wang, Y. Li, X. Zhang, X. Liu, Y. Zhang, W. Zhao, C. Qin, Z. Bakenov, (2020) Vol. 569, 22-33.
- [2] J. Osiak, M. Dwórzniak, *System magazynowania, dystrybucji i sprzedaży biomasy*, Białystok: Towarzystwo Amicus 2015.
- [3] K. Robak, M. Balcerek, *Rola obróbki wstępnej biomasy ligninocelulozowej w produkcji bioetanolu II generacji*, Łódź: Acta Agrophysica 2017.
- [4] T. Mirowski, E. Mokrzyński, A. Uliasz-Bocheńczyk, (2017) Vol. 24, 301-318.
- [5] K. Zamorski, *Współspalanie biomasy w kotle rusztowym (na przykładzie badanego obiektu)*, Gliwice: Energetyka 2006.
- [6] A. Roszkowski, (2012) Vol. 3(77), 79-100.
- [7] P. Kazimierski, P. Hercel, K. Januszewicz, D. Kardaś, (2020) Vol. 13, 3188.
- [8] P. Kazimierski, P. Hercel, T. Suchocki, J. Smoliński, A. Pladzyk, D. Kardaś, J. Łuczak, K. Januszewicz, (2021) Vol. 12, 2969.
- [9] K. Januszewicz, A. Cymann-Sachajdak, P. Kazimierski, M. Klein, J. Łuczak, M. Wilamowska-Zawłocka, (2020) Vol. 13, 4658.
- [10] S. Stelmach, *Piroliza odpadów jako element gospodarki o obiegu zamkniętym*, Gliwice: Wydawnictwo Politechniki Śląskiej 2019.

- [11] P. Kazimierski, M. Klein, D. Kardaś, *Wpływ temperatury na skład produktów pirolizy*, w: *Współczesne problemy energetyki III*, K. Pikoniak, M. Czop (red.), Gliwice: Archiwum Gospodarki Odpadami i Ochrony Środowiska 2015.
- [12] M. Retajczyk, A. Wróblewska, (2018) Vol. 72, 127-146.
- [13] T. Suchocki, P. Lampart, P. Kazimierski, K. Januszewicz, B. Gawron, Ł. Witanowski, (2021) Vol. 2018, 119125.
- [14] K. Januszewicz, P. Kazimierski, M. Klein, D. Kardaś, J. Łuczak, (2020) Vol. 13, 2047.
- [15] M. Marmiroli, U. Bonas, D. Imperiale, G. Lencioni, F. Mussi, N. Marmiroli, E. Maestri, (2018) Vol. 9, 2119.
- [16] N. Tsubouchi, M. Nishio, Y. Shinohara, J. Bud, Y. Mochizuki, (2018) Vol. 176, 76-84.
- [17] K. Yang, J. Peng, C. Srinivasakannan, L. Zhang, H. Xia, X. Duan, (2010) Vol. 101, 6163-6169.
- [18] M.K. Lam, R. Zakaria, *Production of activated carbon from sawdust using sfluidised bed reactor*, International Conference on Environment ICENV 2008.
- [19] K. Biernat, S. Gołębowska, (2010) Vol. 8/2, 23-44.
- [20] L. Czepirski, (2007) Vol. 23, 75-84.
- [21] M. Li, H.B. Huang, R.Z. Wang, L.L. Wang, W.D. Cai, W.M. Yang, (2004) Vol. 29, 2235-2244.
- [22] P. Nowicki, R. Pietrzak, *Węgłe aktywne wzbogacone w azot – otrzymywanie, właściwości i potencjalne zastosowanie*, w: *Adsorbenty i katalizatory Wybrane technologie a środowisko*, J. Ryczkowski (red.), Rzeszów: Wydawca – Uniwersytet Rzeszowski 2012.
- [23] J. Chroma, M. Kloske, (1999) Vol. 2, 3-17.
- [24] H. Marsh, E.A. Heintz, F. Rodriguez-Reinoso, (1997) Vol. 225, 1-10.
- [25] Z. Heidarinejad, M.H. Dehgani, M. Heidari, G. Javedan, I. Ali, M. Sillanpää, (2020) Vol. 18, 393-415.
- [26] A. Ahmadpour, D.D. Do, (1997) Vol. 35, 1723-1732.
- [27] P. Nowicki, J. Kazmierczek, R. Pietrzak, (2015) Vol. 269, 312-319.
- [28] P. Brzozowski, K. Zmarlicki, *Uwarunkowania ekonomiczne w produkcji czereśni i wiśni*, Skierniewice: Wydawca: Instytut ogrodnictwa 2017.
- [29] A.I. Anukam, B.P. Goso, O.O. Okoh, S.N. Mamphweli, (2017) Vol. 2017, 1-9.
- [30] N. Arumugam, S. Anandakumar, (2016) Vol. 6, 9-13.
- [31] B. Barczak, *Influence of the parameters of the waste biomass chemical activation process on the development of the specific surface area of carbon materials*, engineering work, Faculty of Chemistry, Gdansk University of Technology, 2021.
- [32] D. Czarna-Juszkiewicz, M. Wdowin, P. Kunecki, P. Baran, R. Panek, R. Żmuda, (2018) Vol. 107, 19-32.
- [33] M. Hema, S. Arivoli, (2009) Vol. 16, 38-45.
- [34] N. Srilek, P. Aggarangsi, *Physical and chemical characteristics of scarbonised corncob through hydrothermal and pyrolysis conversion*, IOP Conference Series: Materials Science and Engineering, 2021.
- [35] M.G. Lussier, J.C. Shull, D.J. Miller, (1994) Vol. 32, 1493-1498.
- [36] F.O. Erdogan, (2016) Vol. 49:7, 1079-1090.

- [37] J. Kaźmierczak, P. Nowicki, R. Pietrzak, (2012) Vol. 19, 273-281.
- [38] M.R. Haque, J.H. Bradbury, (2002) Vol. 77, 107-114.
- [39] E.N. El Qada, S.J. Allen, G.M. Walker, (2006) Vol. 124, 103-110.
- [40] M. Ghaedi, E. Nazari, R. Sahraie, M.K. Purkait, (2014) Vol. 52, 5504-5512.
- [41] N. Abdolrahimi, A. Tadjarodi, (2019) Vol. 41, 51.
- [42] M. Ryms, K. Januszewicz, P. Kazimierski, J. Łuczak, E. Klugmann-Radziemska, W. Lewandowski, (2020) Vol. 13, 1-18.

DEVICES FOR MONITORING THE TECHNICAL CONDITION OF ENGINE OILS

Tomasz Filipiuk

Faculty of Mechanical Engineering, Military University of Technology, Warsaw, Poland
corresponding author: tomasz.filipiuk@wat.edu.pl

Abstract:

Monitoring the technical condition of engine oils is a very important issue in the aspect of car diagnostics. Based on the quality parameters of fresh and aged engine oil, the condition of the internal combustion engine can be determined. The development of the economy and technical progress in the field of motorization constantly forces changes in the production of engine oils. Currently, very high demands are placed on engine oils. There are many methods that allow you to determine the technical condition of the engine oil. Laboratory methods allow you to carry out very precise tests, however, they are laborious and time-consuming. In the case of on-line methods, it is possible to control the technical condition of the oil on an ongoing basis, however, these methods do not provide precise results.

Keywords:

engine oil, viscosity, aging, monitoring

Introduction

The use of lubricants dates back to antiquity. During the construction of their buildings, the Egyptians used animal and vegetable fats to transport boulders more easily. There are many references to the use of lubricants throughout history. In each case, the idea was that the lubricant had the appropriate characteristics. On the one hand he facilitate sliding relative to each other two elements, the other responsible for maintenance of the components and sealing of various joints. Currently, it is difficult to compare vegetable and animal fats to the lubricating oils used. The development of research and practice allowed for the creation of appropriate mixtures that fulfill a number of functions and allowed them to be used in many friction nodes. Monitoring the technical condition of engine oils is a very important stage in the diagnostic process of oils. Detailed laboratory analysis of both fresh and used engine oil gives a lot of important information, both about the quality condition of the engine oil and the technical condition of the engine. Adequate and precise diagnostics can, on the one hand, ensure the efficient operation of the drive unit, and, on the other hand, reduce fuel consumption and the emission of harmful substances into the atmosphere.

Characteristics of engine oils

Motor oils are a type of lubricating oil that is used in engines to lubricate internal components. The main task of engine oils is to reduce the coefficient of friction between the mating surfaces and to reduce wear and minimize the possibility of corrosion. In addition, they are responsible for cooling the lubricated elements, removing contaminants arising during operation, sealing the lubricated nodes and damping vibrations. In a word, engine oils are responsible for protecting the working components of the internal combustion engine.

Motor oils are designed to fulfill specific tasks in an internal combustion engine. The first essential task is to meet the tribological aspects. They are based on ensuring the functional reliability of all friction areas under all operating conditions. It is important that the engine oil works properly with both low and high loads in the friction junctions. Currently used engine oils have such a wide range of applications that they can be used both at extremely low and high temperatures, and their properties allow the lubricated systems to function properly. In addition to the essential tribological functions, the task of the engine oil is to seal the cylinder and piston and to cool the piston by removing heat from it. In addition, engine oil carries sediments, contaminants, sludge and soot from engine components to the oil filter, where they are separated from the oil. Apart from the aforementioned functions, engine oil should protect engine components against corrosion, and any water that may be present in the lubrication system should be emulsified by the lubricant [1].

In order to ensure the above-mentioned functions and tasks, the engine oil must have appropriate properties which depend to a greater or lesser extent on the elemental composition of the oil. Motor oils consist of an oil base and a number of additives. As a standard, appropriate additives or packages of additives are added to the engine oil, which significantly improve its properties [1, 2]. The use of an appropriate base divides engine oils into mineral, synthetic and semi-synthetic (a mixture of mineral and synthetic bases). Currently, there are about 30 different additives added to base oils [1]. There are the following types of additives [2]:

- viscous;
- antioxidant;
- dispersing washing;
- depressants;
- lubricating;
- przeciwpienne;
- aromatic;
- corrosion inhibitors;
- dyes;
- multifunctional additives.

All the additives used are an indispensable and necessary element in the composition of engine oils. Due to the fact that currently used oils are called multigrade oils, it is necessary to maintain the appropriate viscosity value both at low and high temperatures. For this reason, viscosity additives are very important, as they maintain the appropriate lightness of the oil at low temperatures (basically it happens spontaneously) and allow to maintain the appropriate viscosity at high temperatures.

Aging characteristics of engine oils

The aging of oils is nothing more than the course of changes in the properties of a given product over time. The aging characteristics of engine oils consist in checking how the properties of engine oil have changed after an appropriate operating time in relation to the properties of fresh engine oil. The change in properties is related to the loss of basic oil components and the simultaneous increase in unnecessary components. In the case of basic ingredients, these are base hydrocarbons and additives. During the use of engine oil, the loss of hydrocarbons may occur, which is not a serious problem for the properties of the engine oil, and additives whose task is to improve the properties, which creates certain risks. Loss of additives is a known and natural problem, as a result it leads to the loss of class for a given engine oil and it is necessary to replace it with a fresh one. In addition to the loss of certain substances in the oil, wear products, mechanical impurities, water, fuel and other operating fluids used in the engine are also formed, which in turn also affects the negative assessment of the class of a given oil. Therefore, it is very important to periodically change the engine oil, and an even better solution is to monitor the condition of the oil on the basis of the obtained results describing the parameters of the aging change of engine oils. It is not always necessary to change the engine oil after driving a certain number of kilometers, it all depends on the operating conditions of the engine and the driving culture of the driver. As a result of aging processes, i.e. thermochemical processes and oxidation as well as the formation of external impurities, the chemical composition of fresh engine oil changes, which results in the formation of aged (used) oil Fig. 1.

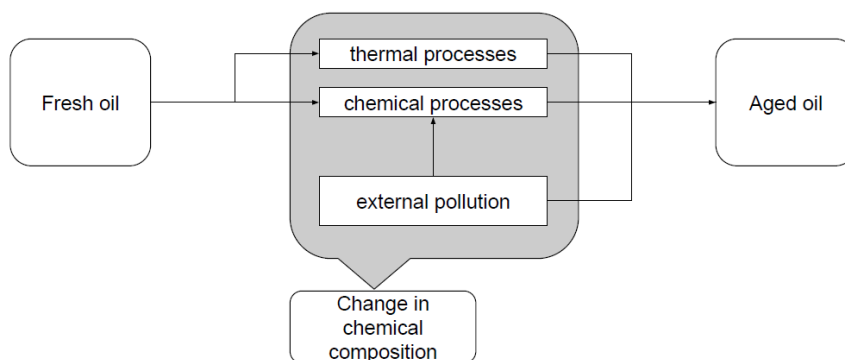


Fig. 1. Changes in the chemical composition of engine oil
Source: [3]

Changes in the chemical composition occur as a result of the factors mentioned in Fig. 1. Thermal and chemical processes always occur as a result of the operating conditions in which the engine oil is used. On the other hand, external pollutants may, to a greater or lesser extent, affect the aging processes, depending on the efficiency of the systems, tightness of connections and the age of the vehicle, engine and its components..

Methods and devices for the assessment of technical condition

Examination of the technical condition of engine oils is the basis for assessing their usability. The analysis of engine oils is based on checking their quality both before use in an internal

combustion engine and after a specified period of use. In practice, the quality of engine oil is not assessed before it is used in a vehicle engine, as the oil manufacturers indicate it on the packaging. However, after the period of use, the used engine oil should be subjected to qualitative and viscosity assessment in order to determine how the properties of a given product have changed and whether this may affect the condition of the engine or fuel system of the vehicle. There are many more or less advanced methods for assessing the technical condition of engine oil. Depending on the needs and conditions, their use is more or less justified and profitable. The technical condition of engine oils is assessed on the basis of quality parameters that can be determined in laboratory conditions as well as on an ongoing basis after taking a sample directly from the place of its use.

One of the methods of assessing the technical condition of engine oil is the use of Fourier transform infrared spectroscopy (FTIR). This method is based on the study of the spectra of chemical compounds with specific bonds of a given, tested substance. Thanks to the use of this method, it is possible to determine the level of engine oil degradation in a relatively short time together with the determination of the content of other liquids in the oil. FTIR analysis allows the determination of contamination, loss of additives, the presence of soot, water, fuel and coolants in the engine oil. Determining this type of substances in engine oil gives a lot of important information showing both the technical condition of the internal combustion engine and the level of oil degradation. However, it should be noted that the FTIR method allows to determine the presence of a given substance in engine oil, however, in order to determine the degree of oil degradation, a series of precise laboratory tests with a thorough analysis of the causes and effects [4]. The infrared spectroscopy method also allows to estimate the acid number (TAN) and base number (TBN) values in used oils [5]. The FTIR method allows you to quickly determine the quality of engine oil. The work [4] shows the evaluation of the quality of engine oils on two devices. Six engine oil samples from different manufacturers of the same lightness class were selected for the test. Samples were subjected to operating on engines of different vehicles and evaluated for oxidation, nitration, the content of carbon black, base number and content of additive expressed as a percentage. The study used an infrared spectrometer. The authors of the study stated that it was possible to determine all parameters assumed before the study. The obtained results made it possible to evaluate the degree of degradation of engine oils in comparison to fresh oil. It was unequivocally stated that the devices, due to their mobility and speed of operation, made it possible to perform the tests. For the test, the samples did not have to be specially prepared and they gave the result almost immediately. These types of devices allow you to use them in the field and determine the time of changing the oil with fresh oil on an ongoing basis. During the FTIR analysis it is possible to quickly determine the technical condition of the internal combustion engine. Unfortunately, as the authors state, the obtained results do not necessarily correspond to the results obtained in specialized laboratory tests, which may indicate the need for additional tests [4, 5].

One of the basic parameters of engine oil is kinematic viscosity, which allows to determine whether a given oil is degraded due to oxidation, contamination or dilution with another product. As a result of oxidation in engine oil, products of high molecular weight are formed, which translates into an increase in the value of oil viscosity. Unfortunately, the value of viscosity as a result of aging may be distorted as a result of dilution with fuel, which in turn translates into a reduction of engine oil viscosity [6]. Laboratory methods of measuring the lightness of engine oil are very well known

and allow to determine the technical condition of the tested product without any major problems. It is possible to monitor the viscosity of the engine oil on an ongoing basis, i.e. on-line methods of monitoring the viscosity. This solution aims to show the technical condition of engine oil in a short time and at limited costs, without the need to perform time-consuming and complicated laboratory tests. High demands are placed on the equipment for monitoring the technical condition of engine oils on an ongoing basis, as they must function for a long time with infrequent calibrations and maintenance, in difficult environmental conditions; high engine temperature. On-line viscometer use to measure lightness of the method of macro-objects, vibration and acoustic methods. In the case of the displacement of bodies on a macro scale, the analogy to laboratory methods is used. A capillary is installed in the engine's oil flow system, which allows the pressure (its drop) to be measured at a fixed flow. Unfortunately, the result may be affected by impurities in the capillary after a longer period of use and the fact that the oil flow in the engine is not constant, but changes depending on the operating conditions. The devices used to monitor the viscosity of engine oil on an ongoing basis include: Brookfield rotational viscometer, a falling piston viscometer and an electromagnetic viscometer, which uses in its structure the movement time of a piston placed between two electromagnetic coils [7]. Other ways to measure the viscosity of engine oil on-line are methods based on vibration and acoustics. In this case, no moving parts are used that can move and may wear or even be damaged. In the case of vibrating devices, the dynamic viscosity of the engine oil is checked on the basis of the phase difference between the vibrating signal from the vibrating device and the natural vibration signal of the device. Acoustic viscometers are based on the transmission of waves through a liquid. On one side of the oil pipe there is an acoustic wave generator, which induces an acoustic wave in the liquid, and on the other side, a receiver whose task is to receive the propagating wave by the liquid. The main problem of this type of viscometers is the fact that the speed of the acoustic wave does not only depend on the viscosity of the liquid, but also on the contamination with wear products and the presence of air bubbles [7].

An important aspect in the examination of the technical condition of the lubricant is the content of soot in the oil as a result of working in the internal combustion engine. There are many laboratory methods to check the soot content of the engine oil. These methods relate to thermogravimetric analysis, infrared, sedimentation, Blotter, and photon correlation spectroscopy. Thermogravimetric analysis is based on an accurate measurement of the soot content expressed as a percentage by mass. Infrared analysis is a fast and relatively well developed method. Its use is absolutely wide and most suitable for the determination of soot in engine oil. A disadvantage is the increase in infrared radiation absorption, which is due to the increase in the size of the soot particles. Engine oil sedimentation is based on the separation of insoluble substances from those that are dissolved. The disadvantage of this method is that everything that does not dissolve is weighed, and in addition the type of solvent chosen to dilute the oil can have a big influence on the result. The Blotter method is based on the determination of the insoluble substances by visual method after applying a small sample of oil to chromatography paper. This analysis is simple, relatively quick, however, it does not provide information on the amount of the substance, but only allows to determine the presence of soot in the oil. Photon correlation spectroscopy is a relatively complicated method. This method uses dynamic scattering of laser radiation. Thanks to this, it is possible to determine the size of the distribution of soot particles contained in the engine oil [8].

Unfortunately, it is important to have real-time information about the technical condition of the oil in order to keep your engine in top shape. For this purpose, there are several methods and devices for monitoring the technical condition of engine oils installed in motor vehicles. The currently used devices for monitoring the presence of soot contained in engine oils are carried out using optical and electrical methods. Electrical methods are based on the measurement of electrical conductivity and permeability, which change due to the consumption of oil in the vehicle's engine. Fresh engine oil is characterized by high electrical resistance and low permeability. Along with soot contamination of the engine oil, the indicated parameters change. Electrical methods can be applied by integrating appropriate devices into the lubrication system. The general structure of the electric sensor for measuring soot in engine oil is shown in Fig. 2.

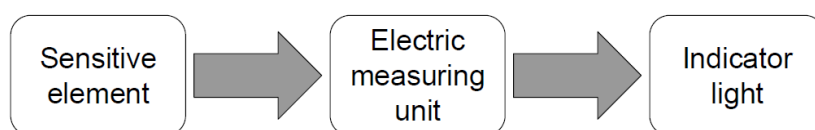


Fig. 2. Schematic diagram of the construction and operation of electric devices for determining the soot content in oil
Source: [8]

The principle of operation is based on the measurement of resistance by an electrical measuring unit through a signal received from a sensitive element consisting of electrodes. As the soot content in the oil increases, the resistance between the electrodes decreases, which translates into an increase in the conductivity of the oil. When the soot concentration in the oil reaches a critical level, the signal lamp [8] lights up. This solution is very sensitive to electrical noise, so it is more advantageous to measure the total conductivity of the engine oil using an alternating current rather than a direct current.

In the case of optical devices, an important aspect is to ensure a short and constant optical path, and the oil flow should be through a narrow aperture. The measurement is based on the absorption of optical radiation, which in this case depends mainly on the soot contained in the oil. Due to the fact that water, coolants and fuels have a lower absorption coefficient, their content in the engine oil does not affect the result of the soot content measurement. The measurement of the soot content in the engine oil can be done using a photometric device where two plate-convex lenses are in contact with each other in the oil. The corresponding diode produces radiation that is focused on the photodetector, after amplifying the signal, the radiation is transferred to the voltage indicator, which converts the voltage to the concentration of soot in the oil using a calibration graph. Another way to keep the optical path constant is to use the principle of total internal reflection between the optical material and the oil under test. This is based on the absorption of the radiation after passing through a layer of a certain thickness and refractive index. In this case, the main disadvantage is that after some time the surface of sensitive measuring elements becomes contaminated, which may result in distortion and false results [5].

Currently, there are a lot of devices and laboratory devices that allow you to monitor the technical condition of engine oils. Laboratory methods allow you to perform a number of tests and determinations with relatively high precision, but they provide information about the condition of the oil only after some time. The test methods provide the result on an ongoing basis while the engine is

running, while driving, however, they are not always able to reflect the actual condition due to design constraints and difficult working conditions.

Conclusions

The presented paper is based on the presentation of modern equipment to monitor the status of motor oils. The subject area is very extensive and a detailed analysis is related to many aspects. The proposed development is designed to give general information related to the topic and not the detailed develop. Summarizing the aspects discussed in the study, the following conclusions can be made.

1. Due to their properties and composition, engine oils have a wide range of applications and can be used depending on the needs in various types of friction nodes that occur in internal combustion engines.
2. During the use of oil in a vehicle engine, a number of processes and changes in properties take place, as a result of which an aged engine oil is formed, which after a certain period of use (mileage) loses its properties and must be changed to fresh oil.
3. There are many methods of monitoring the technical condition of engine oil, both in laboratory conditions and on an ongoing basis in the vehicle's engine lubrication system.
4. FTIR analysis allows to indicate changes in the properties of engine oils by determining the presence or not of a given chemical compound, unfortunately, when determining the content of the aging product in the oil, thorough and precise tests and laboratory analyzes are required.
5. When measuring the kinematic viscosity on-line, it is possible to quickly measure this parameter, but to a large extent, dilution with other substances may lower the result and only laboratory measurements are able to accurately determine the level of engine oil degradation.
6. In the case of measuring the soot content in engine oil, the main problem at present is to make sensitive elements with appropriate coatings, which are able to ensure a longer operation time of the devices in the condition of test cleanliness.

Practically speaking, the device and methods of research related to the determination of the technical state of motor oils is associated with one hand with the measurement date and the determination of quality changes and the viscosity directly in the operation of the vehicle, however, identify the causes and possible effects is related fundamentally to the performance of accurate and time-consuming research and analysis in laboratory conditions.

Literature

- [1] M. Harperscheid, Engine Oils, In: Mang T. (eds) *Encyclopedia of Lubricants and Lubrication*, Springer, Berlin, Heidelberg 2014, 487-492.
- [2] K. Baczewski, P. Szczawiński, W. Zielnik, *Płyny eksploatacyjne, Wstęp do zajęć laboratoryjnych*, Wojskowa Akademia Techniczna, Warszawa 2010, 149-200.
- [3] A. Wachal, K. Biernat, *Materiały pędne i smary*, Wojskowa Akademia Techniczna, Warszawa 1985, 280-282.

- [4] A. Wolak, G. Zając, *Changes in the operating characteristics of engine oils: A comparison of the results obtained with the use of two automatic devices*, Measurement, Vol. 113, 2018, 56-61.
- [5] V. Macián, et al., *Applying chemometric procedures for correlation the FTIR spectroscopy with the new thermometric evaluation of Total Acid Number and Total Basic Number in engine oils*, Chemometrics and Intelligent Laboratory Systems, Vol. 208, 2021, 1-8.
- [6] A. Mujahid, t F. L. Dicker, *Monitoring automotive oil degradation: analytical tools and onboard sensing technologies*, Analytical and Bioanalytical Chemistry, Vol. 404, 2012, 1197-1209.
- [7] N.K. Myshkin, L.V. Markova, *Oil Viscosity Monitoring, In: On-line Condition Monitoring in Industrial Lubrication and Tribology*, Applied Condition Monitoring, Springer, Vol. 8, 2018, 31-59.
- [8] N.K. Myshkin, L.V. Markova, *Control of Soot Concentration in Oil. In: On-line Condition Monitoring in Industrial Lubrication and Tribology*, Applied Condition Monitoring, Springer, Vol. 8, 2018, 83-129.

3D PRINTING WITH MIXES WITH HIGH-ALUMINA CEMENTS – STATE OF ART

Natalia Gierszewska*, Jakub Uciurkiewicz, Jarosław Błyszko

Department of Reinforced Concrete Structures and Concrete Technology, Faculty of Civil and Environmental Engineering, West Pomeranian University of Technology in Szczecin, al. Piastów 50a, 70-311 Szczecin, Poland

**corresponding author: gn47140@zut.edu.pl*

Abstract:

3D printing is the new, alternative method for creating concrete constructions. Nowadays it is more and more often used instead of current technologies. This modern method also appears to be more efficient than the ones used until now. Materials, which are used for three-dimensional printing, must fulfill requirements from standards, just as materials used in conventional execution. In this article it is described which specific requirements should the concrete mixture fulfill to be used in 3D printing and what are the opportunities of using this method. Furthermore, in the article there are included restrictions for materials used in 3D printing such as maximum height of the printed element. Another aspect appearing in the article concerns high-alumina cements as an alternative binder in the concrete mixture. This paper presents selected aspects of the use of high alumina cement in 3D printing.

Keywords:

high alumina cement, 3d printing, cement mixture

Introduction

In the structural design over the past several years it is endeavoured to automate and computerize the erection of the constructions as much as it is possible. Three-dimensional printing is becoming one of the most popular methods which are being developed nowadays. It is required to be more beneficial in the aspect of economics when the duration of the execution and the use of additional materials are considered. However, it must meet specific requirements and restrictions to bring the most efficient results. It is also important to consider all important factors when deciding on the method which will be used in the given project.

In 3DCP technology constructions are created by the head that moves according to a predefined trajectory and creates a construction by layers. It is important that the freshly extruded layer of concrete connects with the previous one at the exact time to let the concrete gain enough strength to endure the weight of the upcoming layers but also before it gets too dry to connect with the upper layer. With this technology both prefabricated elements (e.g., stairs, ceilings, roofs) and on-site structures or even the whole buildings can be erected [1]. There exist many different methods of three-dimensional printing and they are used depending on the type of the structure, its size or type

of stresses appearing in the element. 3D printing with fast-setting mixes in the future could also be used for emergency strengthening of structures or soil foundation [2]. The future of 3D printing also includes targeted applications using highly specialized compounds modified with nanomaterials [3] [4]. Printing successive layers too quickly destroys the structure. Research is currently being conducted to speed up the printing process while eliminating the problems of shrinkage and structure collapse. An example of a Cartesian printer for cementitious materials is shown in Fig. 1. Fig. 2 shows an example of defects in the printed structure.

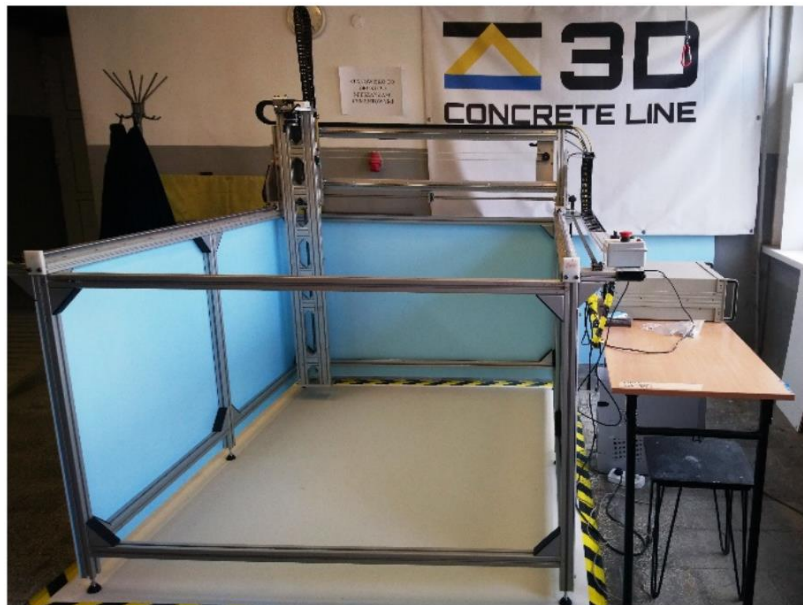


Fig. 1. 3D printer for printing with cementitious materials. Workspace 1.40 x 1.40 x 0.80 m
Faculty of Civil and Environmental Engineering in Szczecin
Source: author's own study

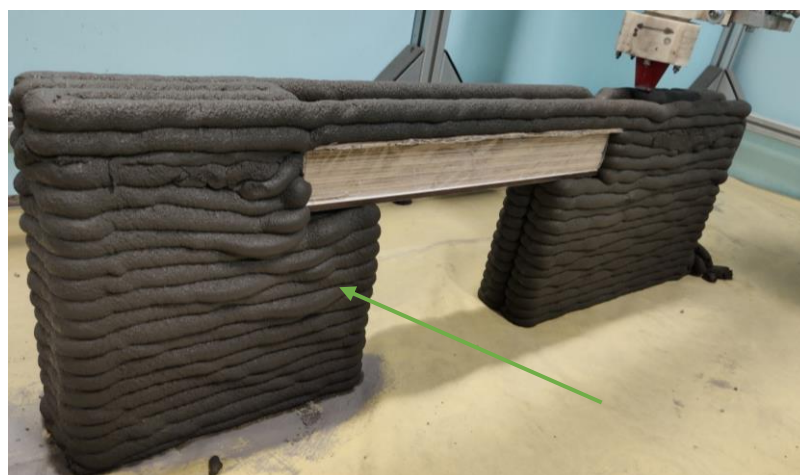


Fig. 2. Printing defects
Source: author's own study

Requirements of materials

Materials used for 3D printing must be tested for fresh state properties such as buildability, extrudability, flowability and open time. These parameters determine the appropriate endurance of a concrete mixture and its behavior during the whole printing process [5].

Buildability

The concrete layer in 3D printing must withstand its own weight straight after being extruded from the head. The created structure must also sustain the load of upcoming layers without causing any failure. That is why the samples during the research must be tested for strength in compression. The buildability of element printed in 3DCP technology depends on the shear yield stresses, green strength and elastic modulus. Another important factor is the buckling failure [6]. The printed element must resist against deformations which is, due to lack of any formwork, harder to accomplish than in traditional technologies. Thus, determination of fresh state elastic modulus of the material is necessary.

Pumpability and extrudability

The pumpability and extrudability are the abilities to be pumped and extruded out of the head of the printing machine properly. On these properties influence the consistency of the material which means the amount of water, cement, aggregate and additional ingredients. Also, cohesiveness, stability, rheology of concrete and probability of phase separation during the application process. In general, the mix pumped to the head cannot be too dense or rare, it also should consist of enough amount of cement to prevent separating water from the rest of the mix during extruding layers. It is important for the mix to smoothly move inside the pump and avoid a blockage of it.

Flowability

Flowability is closely related to the extrudability of the material. It is basically the ability of the concrete mix to flow through all the pump without any troubles such as blockages, ingredients separations or outflows when it is not desired due to too rare mixture. The usage of different granulation of aggregate allows denser packing of the mix grains and in this way enhance the mixture's fluidity in the printing tube. It is important to use the appropriate amount of dusty fraction. There cannot be too much of this fraction, because the smaller grains have bigger specific surface area, thus they absorb more water. To determine flowability of the material it is required to create an accurate consistency of the mixture. In this regard the flow table test is performed. It is also crucial when the open time of the mixture is considered. With the flow table test it is first checked if the sample has proper shape after removing the form on the table. Afterwards, the sample is exposed to a regular vibration and then the diameter of the resulted shape is measured.

Open time

In the created concrete mixture, the rheological properties must be kept for the concrete to maintain its shape during extruding it from the head. It is also connected with the extrudability and pumpability of concrete. It is important to create the exact setting time for the mixture – both the beginning and the end of it. The moment when the extruded layer connects with the former one, must

be before the start of setting time, because otherwise it would become denser already in the tube and therefore cause slower flow of the mixture through it. On the other hand, the new layer needs to already create the bindings with the lower layer. Furthermore, it cannot spread after being applied to the construction. The layer that is being covered with the following one, must also endure the weight of the concrete above without buckling or other damages. Thus, in the previously laid layer the setting time must already begin. Moreover, the concrete must be applied before the end of setting time so the bindings can be easily created to connect all the layers in one load-bearing structure.

Limitations concerning concrete mixes in 3DCP technology

Despite all the advantages of three-dimensional printing technologies, there are also fields, where it cannot be used, or the alternative way should be implemented. This happens e.g., when elements of stairs, ceilings, cantilevers, or too high walls need to be erected. There are also limitations for particularly large buildings. In these situations, the solution for the problem can be the prefabricated element. Elements of stairs, ceilings or cantilevers can be produced in the laboratory and afterwards transported to the building site [7]. Unfortunately, this implies necessity of using special machinery, which in consequence leads to the raise of costs during execution process.

Printed thin-walled parts have a large drying area. Shrinkage of such compounds and methods of care are of interest to researchers. Shrinkage reduction is designed by appropriate curing conditions or additives [8, 9].

Usage of high-alumina cement in 3D printing mixes

The alumina cement in combination with Portland cement has big impact on the setting time. When using from 20% to 80% of one of the mentioned cements in the concrete mixture, it appears to shorten setting time to minimum. In the research described in the second article [10], the purpose was to control setting time to start and end at the exact time, when the concrete is extruded from the head on the existing layer. For the research, the alumina cement GÓRKAL 40 and GÓRKAL 70 and Portland cement CEM I 42,5 R were used. They were tested in combination of Portland cement with 15% to provide extra time to pump and extrude the mixture from on the structure but also to accelerate the hardening period after the layer is applied to avoid spread of concrete and later – failure. Furthermore, the purpose of adding alumina cement is to decrease the amount of admixtures to minimum but with keeping similar properties of the mixture.

Acknowledgements

This research was supported by ZUT Highfliers School (Szkoła Orłów ZUT) project, co-ordinated by Dr. Piotr Sulikowski, within the framework of the program of the Minister of Education and Science [Grant No. MNiSW/2019/391/DIR/KH, POWR.03.01.00-00-P015/18], co-financed by the European Social Fund, the amount of financing PLN 1,704,201,66.

Literature

- [1] Mostafa Y., An C., *Applicability and Limitations of 3D Printing for Civil Structures* (2015). Civil, Construction and Environmental Engineering Conference Presentations and Proceedings. 35, http://lib.dr.iastate.edu/ccee_conf/35
- [2] Hoffmann, M.; Żarkiewicz, K.; Zieliński, A.; Skibicki, S.; Marchewka, Ł. *Foundation Piles-A New Feature for Concrete 3D Printers*. Materials (Basel) 2021, 14, doi:10.3390/ma14102545.
- [3] Federowicz, K.; Techman, M.; Sanytsky, M.; Sikora, P. *Modification of Lightweight Aggregate Concretes with Silica Nanoparticles-A Review*. Materials (Basel) 2021, 14, doi:10.3390/ma14154242.
- [4] Federowicz, K.; Figueiredo, V.A.; Al-Kroom, H.; Abdel-Gawwad, H.A.; Abd Elrahman, M.; Sikora, P. *The Effects of Temperature Curing on the Strength Development, Transport Properties, and Freeze-Thaw Resistance of Blast Furnace Slag Cement Mortars Modified with Nanosilica*. Materials (Basel) 2020, 13, doi:10.3390/ma13245800.
- [5] Kruger, J.; Zeranka, S.; van Zijl, G. *3D concrete printing: A lower bound analytical model for buildability performance quantification*. Automation in Construction 2019, 106, 102904, doi:10.1016/j.autcon.2019.102904.
- [6] Jayathilakage, R.; Rajeev, P.; Sanjayan, J.G. *Yield stress criteria to assess the buildability of 3D concrete printing*. Construction and Building Materials 2020, 240, 117989, doi:10.1016/j.conbuildmat.2019.117989.
- [7] Duballet, R.; Baverel, O.; Dirrenberger, J. *Classification of building systems for concrete 3D printing*. Automation in Construction 2017, 83, 247–258, doi:10.1016/j.autcon.2017.08.018.
- [8] Skibicki, S.; Kaszyńska, M.; Wahib, N.; Techman, M.; Federowicz, K.; Zieliński, A.; Wróblewski, T.; Olczyk, N.; Hoffmann, M. *Properties of Composite Modified with Limestone Powder for 3D Concrete Printing*. In Second RILEM International Conference on Concrete and Digital Fabrication; Bos, F.P., Lucas, S.S., Wolfs, R.J., Salet, T.A., Eds.; Springer International Publishing: Cham, 2020; pp 125–134, ISBN 978-3-030-49915-0.
- [9] Federowicz, K.; Kaszyńska, M.; Zieliński, A.; Hoffmann, M. *Effect of Curing Methods on Shrinkage Development in 3D-Printed Concrete*. Materials (Basel) 2020, 13, doi:10.3390/ma13112590.
- [10] Bhattacharjee, S.; Basavaraj, A.S.; Rahul, A.V.; Santhanam, M.; Gettu, R.; Panda, B.; Schlangen, E.; Chen, Y.; Copuroglu, O.; Ma, G.; et al. *Sustainable materials for 3D concrete printing*. Cement and Concrete Composites 2021, 122, 104156, doi:10.1016/j.cemconcomp.2021.104156.

THE PERCEPTION OF SEXUAL MINORITIES IN POLAND IN SURVEYS

Natalia Kawiak

Faculty of Education, Institute of political science and administration, Jesuit University Ignatianum in Krakow
corresponding author: nataliakawiakk@gmail.com

Abstract:

The main aim of my paper was to research how sexual minorities are perceived in Poland and how their social situation is shaped. In order to illustrate it, two types of research were conducted – survey and focus group studies. I also conducted the overview of the selected subject literature in order to enrich my analyses with a broader context.

Keywords:

sexual minorities, tolerance, homophobia

Introduction

In Poland acts discriminating people belonging to sexual minorities occur every day. People come across acts of psychological violence almost on a daily basis. Despite the fact that WHO (World Health Organization) deleted homosexuality from the list of diseases and disorders [1] on 17 May 1990, many people perceive homosexuality and other orientations different from heterosexuality as a disease or disorder. Non-heterosexual people are discriminated at school, at work, in the street and among their friends. Gays, lesbians, bisexual and transsexual persons are often afraid of coming out since they do not want to become the object of jokes or malicious remarks. Polish society is in majority conservative and traditional in their attitude to religion and when it comes to the role of religion in the social-political life. That is why I decided to conduct research concerning how we perceive people with their orientation different from the one that is dominant in Poland and to illustrate the social situation of these people. The research problem is mainly addressed to young people (aged 19-30) since these are people at this age who are most often seen in the streets during Equality Marches and other initiatives of this kind. This is also a group, which in the future, will become the major factor shaping the country's policy in this area.

Bibliography overview

In October 2016 the German company Dalia Research conducted the research aiming at determining the number of people identifying themselves as non-heterosexual persons in European countries. Such research was difficult to conduct due to the fact that Census of Population does not include a question concerning sexual orientation. A significant number of respondents would

probably find such question as too personal. It was concluded that respondents would be more willing to answer honestly if the survey was anonymous. Thus, the survey was conducted with the use of technology for carrying out anonymous surveys with access to the Internet, such as phone or tablet. The survey was completed by 12 thousand people in 28 countries. Dalia Research asked two following questions:

1. Do you identify yourself as a lesbian, gay, bisexual or transsexual person? (Yes / No / I prefer not to answer).
2. Which of the below options best describes your sexual orientation? (Only transsexual persons / Mostly heterosexual persons / Heterosexual and homosexual persons / Mainly homosexual persons, less frequently heterosexual persons / Only homosexual persons / Asexual persons / I prefer not to answer).

Research results show that 4.9% of Polish citizens identify themselves as non-heterosexual persons, belonging to the LGBT society [2]. The overall result of 4.9% people in Poland identifying themselves as people belonging to the LGBT society seems relatively low (7.4% in Germany). It has to be understood that it is only 12 thousand people from 28 European countries who took part in the research, out of which the considerable number of people refrained from providing the reply, which means that the percentage is much larger that the research proves. Many people are afraid or ashamed of talking about their orientation for fear of the bad reaction from society, e.g. being ridiculed or humiliated. As a result, we are not capable of precisely determine the number of non-heterosexual people in Poland. It is possible that we are even not able to calculate the approximate number.

One of the publications of the Campaign Against Homophobia: *Social situation of LGBT people in Poland. Report for 2015-2016* discloses what percentage of people belonging to the LGBT community experienced physical or psychological violence. On the basis of this data, conclusions can be drawn concerning how non-heterosexual people are perceived in Poland. The research results illustrate as follows: 68.9% of LGBT people experienced at least one kind of violence, 63.72% of LGBT people experienced verbal violence, 33.96% of people belonging to the LGBT society experienced threats, 12.84% of non-heterosexual people had contact with physical violence, and 14.11% of people experienced sexual violence. 69.4% of LGBT teenagers had suicidal thoughts, and 49.6% experienced depression. 50% of LGBT people hide their orientation from neighbours and tenants, 71% - at the workplace, and 73.3% - at school or at university [3]. When analysing this research, it can be concluded that people belonging to sexual minorities have to fight for acceptance and tolerance, since not all people are in favour of them. Contrary to Article 32 Section 2 of the Constitution of the Republic of Poland, which states that "No one can be discriminated in political, social or economic life due to any reason" [4] non-heterosexual persons experience acts of discrimination from their peers, family members, friends, as well as strangers, which has an impact on their mental health.

In the article entitled *Prejudice fuels reluctance towards LGBT people* by Navi Pillay dated 4 July 2014, the author of the text states that the rights that enable to punish and deprive homosexual people of their voice are an example of basic human rights violation. Pillay lists many countries where homosexuality is sanctioned with imprisonment, and even with death penalty. The following countries are included in this list: Saudi Arabia, Nigeria, Uganda, Gambia, Kenya, the Democratic Republic of Congo and Brunei. It is obviously not a complete list of countries where such penalty for

homosexuality applies. The author claims that dealing with the 'problem' of gays and lesbians is a deliberate tactic in order to divert attention from real problems, such as poverty. Ignorance and a commonly held view that homosexuality is connected with pedophilia and unhealthy interest in kids foster homophobia and prejudices related to the topic of people from the LGBT society. The author of this article believes that discrimination on grounds of sexual orientation is unfair in the same way as discrimination on grounds of religion or skin colour. In order to fight with the lack of tolerance, the author together with a group of other people initiated the United Nations campaign - *Free&Equal*, the aim of which is to increase the awareness of rights of LGBT people [5]. It is a great and well thought-out initiative, and perhaps thanks to such action promoting the wider knowledge concerning people from the LGBT society more people will be more knowledgeable in this topic. The knowledge concerning this topic is still definitely insufficient today and needs to be broadened. It is probable that thanks to initiatives of this kind, the level of tolerance will increase.

Focus group research – analysis and conclusions

Focus group research was conducted in the group of ten respondents, who answered several questions. The research shows that the term "*sexual minorities*" is understood by respondents as the society of homosexual and bisexual persons, without taking into account transsexual persons. Part of this group does not have contact with non-heterosexual persons in their everyday life, which may be the reason of their scarce knowledge concerning this topic. The second reason of their lack of the correct understanding of *the LGBT community* may be the environment of respondents. People who have daily contact with non-heterosexual persons, have mainly contacts with homosexual and bisexual men and women. There are no transsexual persons in the environment of the people researched, which may result in their limited knowledge concerning this topic. Each respondent considers himself/herself a tolerant person who accepts LGBT people. For all people taking part in the research, sexual orientation is of no importance when developing new friendly relationships; as they indicate – these are personal traits of character count. Each person surveyed states that people themselves from sexual minorities are not problematic for them, yet they have reservations regarding certain behaviours, for example in Equality Marches, i.e. all types of provocations, profanations and excessive display of the body in marches of this type. Another issue raised by respondents is the fact that people from the society of sexual minorities involved Church into the battle for their rights. As one of the respondents claims "Believers, already from the grounds of their faith, should show tolerance towards such people and not harm them. Yet, how can we talk about respect when some LGBT people demolish churches and do not show respect towards other people themselves. It seems to me that the problem lies not in the fact that no one reaches out to them first, neither the Church, nor people from sexual minorities." There is controversy concerning the rights of people from sexual minorities to enter into marriages and to adopt kids. One group, relating to their faith, thinks that it is unacceptable since it is a man and a woman who are the basis for the family. Another group of people think that it is better that a child from a Foster Home had two women or two men as parents, rather than having no parents at all. They claim that such family is better than no family at all, and same-sex parents will pass on kids the same values as parents of both sexes. According to people taking part in the research, people constituting the society of sexual minorities deserve the tolerance in the same

way as any other human being. Each individual deserves respect and being equally treated. They argue that there is a need for social acceptance in Poland, since currently there is no social acceptance at all. According to the respondents, creating campaigns and organisations in order to fight with homophobia is necessary to help the victims and give them support after the harm that they experienced. It seems that here is no discrimination towards people belonging to sexual minorities among respondents, which does not mean that it does not exist in Poland. As people taking part in the focus group research claim, Poland is not ready yet for legalising marriages between people of the same sex or for allowing them to adopt kids. There are no sufficient sources of knowledge concerning this topic and the majority of the Poles draw their knowledge from media. Another reason may be the lack of the proper sexual education in our country. Despite the existence of the school subject Preparation for Family life, you cannot learn much about your sexuality from this subject. There are many taboo topics in Poland, i.e. politics, money, sex or sexuality. According to the respondents, we should fight it and start talking about such topics, which would result in the increased tolerance in our society.

Report from surveys

The total of 90 people took part in the survey. The survey consisted of closed questions with the possibility of a single-choice. The survey was anonymous and it was carried out online in the Microsoft Forms platform. The aim of the questionnaire was to research whether age and sex have any impact on perceiving and tolerance of sexual minorities in Poland.

Fig. 1 illustrates the age of respondents. The vast majority of people taking part in the survey were 19-30 years old, which constituted 84.4% of the total researched.

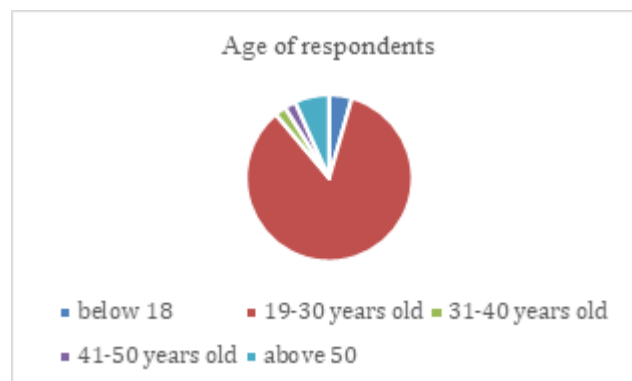


Fig. 1. Age of respondents
Source: Own calculations

The age of the remaining part of respondents presented as follows: people at the age of below 18 constituted 4.4% of the total (4 persons), people aged 31-40 constituted 2.2% of the total (2 persons), people aged 41-50 also constituted 2.2% of the total (2 persons), whereas people at the age of above 50 constituted 6.7% of the total group researched (6 persons).

Fig. 2 shows whether the given people consider themselves as tolerant.



Fig. 2. Tolerance
Source: Own calculations

88.9% (80 persons) of all people researched consider themselves as tolerant, out of whom 75 persons (83.3%) are aged between 19 and 30. Three people are below 18 years of age, and two persons are aged 31-40. 11.1%, i.e. 10 people consider themselves as non-tolerant, out of whom six people (6.6%) are aged above 50 years old, one person is aged between 19 and 30, one person is below 18. The remaining two persons consider themselves as non-tolerant are aged 41-50 and constitute 2.2% of the whole.

Fig. 3 illustrates the gender of people taking part in the survey.

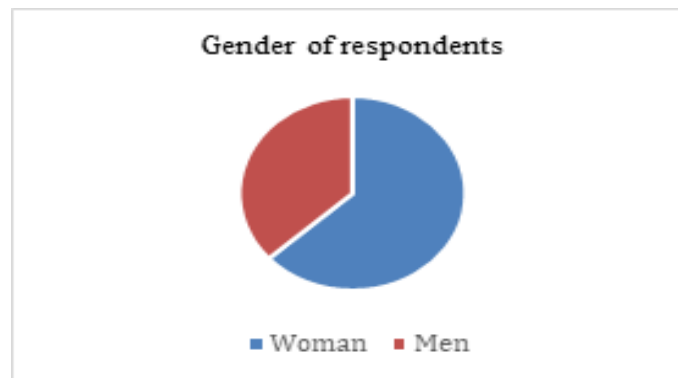


Fig. 3. Gender of respondents
Source: Own calculations

57 women took part in the survey, which constitutes 63.3% of all people taking part in the survey and 33 men took part in the survey, which constitutes 36.7% of the total number of respondents. 51 women (56.6%) and 29 men (32.2%) replied positively when asked "Do you consider yourself to be a tolerant person?". 6 women (6.6%) and 4 men (4.4%) replied negatively when asked this question.

Summary and conclusions

The topic of sexual minorities has been the taboo topic for many years and the one that is reluctantly discussed. Most probably it is rooted in the fact that Poland is the country, whose citizens declare to be Catholics in majority. This means that a family consisting of a man and a woman is perceived as normality by the Poles. Research shows that the term "*sexual minorities*" is misinterpreted by respondents since according to them it is the society that consists only homosexual and bisexual persons. The conducted research shows that there are many factors that have or may have impact on the perception of people from the society of sexual minorities. One of them is faith. Respondents referring to their faith and to being a Christian, concluded that all people should be respected and tolerated, irrespective of their race, colour of the skin, religion or sexual orientation, since the Bible orders to respect every human. Age is the following factor. Research proves that young people (up to 30 years of age) are definitely more tolerant than older people (above 30 years of age). Most likely, it is related to the fact that the younger generation is more open and more tolerant. Older persons also had less contact with people of orientation other than heterosexual. In the past, this topic was not as openly discussed as today, and it is a novelty to them. Behaviours such as profanations, provocations, excessive undressing or vulgar slogans in posters used in Equality Marches efficiently discourage people from respecting non-heterosexual people, since they are associated mainly with such events. Such behaviours have impact on the diminishing group of tolerant people. Research illustrates that sex of respondents has no impact on whether a person is tolerant or not. Being tolerant or not depends wholly on us – it is our personal choice. It is us who decide how we perceive sexual minorities. The perception of sexual minorities by a given person is largely related to the family in which the person was raised, among what people the person lived and what values his parents conveyed him/her and what opinions and beliefs they instilled in him/her. Homophobia and discrimination due to sexual orientation has long been and most probably will be the main reason of all demonstrations and protests for the long time. The level of tolerance has considerably increased for the past couple of years. We have learned our respondents' opinions and values, together with their objections to certain behaviours of sexual minorities mentioned above. It seems that the indicator of tolerance will significantly increase in the future since there are more and more people addressing this topic.

Literature

- [1] *LGBT Encyclopaedia*
https://www.encyklopedia.edu.pl/wiki/Usuni%C4%99cie_homoseksualizmu_z_list_chor%C3%B3b
- [2] *Dalia Research*
<https://daliaresearch.com/blog/counting-the-lgbt-population-6-of-europeans-identify-as-lgbt/>
- [3] *Research on the Campaign Against Homophobia*
<https://kph.org.pl/wp-content/uploads/2015/04/Sytuacja-spoleczna-os%C3%B3b-LGBT-w-Polsce-raport-za-lata-2015-2016.pdf>

- [4] *The Constitution of the Republic of Poland*
[http://www.sejm.gov.pl/prawo/konst/polski/2.htm#:~:text=32.,lub%20 gospodarczym%20 z%20 jakiegokolwiek%20 przyczyny](http://www.sejm.gov.pl/prawo/konst/polski/2.htm#:~:text=32.,lub%20gospodarczym%20z%20jakiegokolwiek%20przyczyny)
- [5] *Navi Pillay, Prejudice fuels reluctance towards LGBT people*
<http://www.unic.un.org.pl/aktualnosci/uprzedzenia-podsycaja-niechec-do-osob-lgbt---artykul-navi-pillay/2586#>

VEO WEATHER ROUTING – AN INNOVATIVE ALGORITHM FOR CALCULATING ROUTES BASED ON WEATHER, MAP AND POLAR PLOTS OF YACHTS

Andrzej Kępys, Ernest Syska*

VEO Sp z o.o.

*corresponding author: ernest.syska@veo.glass

Abstract:

The article demonstrates the adaptation of the Dijkstra algorithm to the marine navigation called VEO Weather Routing. This mechanism is used to solve the problem of determining the sea route in terms of weather data, navigable characteristics of the yacht - with automatic avoidance of land with high efficiency and precision. The full calculation procedure in both phases of the algorithm's operation was presented. As a result, a significant time gain was proved on the route marked with the use of the constructed mechanism in relation to the route marked by hand.

Keywords:

Weather Routing, Marine Navigation, Dijkstra algorithm

Introduction

Mapping the route of a sailing yacht based on weather data has long been an important issue in the practice of sailing. So far, this task has been carried out mainly on the basis of planning "in the head" of the yacht captain, i.e. weather data and the sailor's knowledge / intuition regarding the use of wind and sea currents by a specific ship model. The mathematical, algorithmic version of determining sea routes was known more in the racing world, where every mistake results in a worse result in the race. So far, isochrone algorithms have dominated in regattas and tourist applications. These algorithms are executable on low power computers but have a number of functional limitations. Namely, they do not bypass the complex coastline - and if they have workarounds for this problem, they lose the quality of the designated routes or stop working altogether.

In the near future, the use of algorithms for determining sea routes in the standard navigation activities of the captain of the yacht will be popularized. As was the case with Google Maps and land navigation, the mathematical basis of this process will be Dijkstra's algorithms. The Dijkstra algorithm, however, must be adapted to the issues of maritime navigation. Such an algorithm is VEO Weather Routing presented in this article. The logic of Dijkstra's procedure in the VEO system allows much better avoidance of land and zones excluded from water traffic, while gaining very high accuracy in terms of the size of the geographic square to which the ship is heading. This is at the

expense of the computing power of computers, in this case high-performance graphics processing unit computers.

Theoretical basis

The main tool used in determining the routes is the so-called Dijkstra's algorithm [1]. It is used to determine the shortest path in a graph including all nodes - starting from the first node (source) or to determine the shortest path between two nodes.

Dijkstra's algorithm divides the set of graph vertices into three sets: V, Q, S. The first of them V is the set of all nodes in the graph. Q is the set of all vertices sharing an edge with the source node. The node from the set Q with the shortest path from the center goes to the set S, and then it transforms into the middle node, and the original source node is no longer included in the further operation of the algorithm. The algorithm ends when the set Q is empty or when it reaches a previously defined node.

Dijkstra's algorithm for determining the route between two nodes in the graph can be described on the following example – Fig. 1.

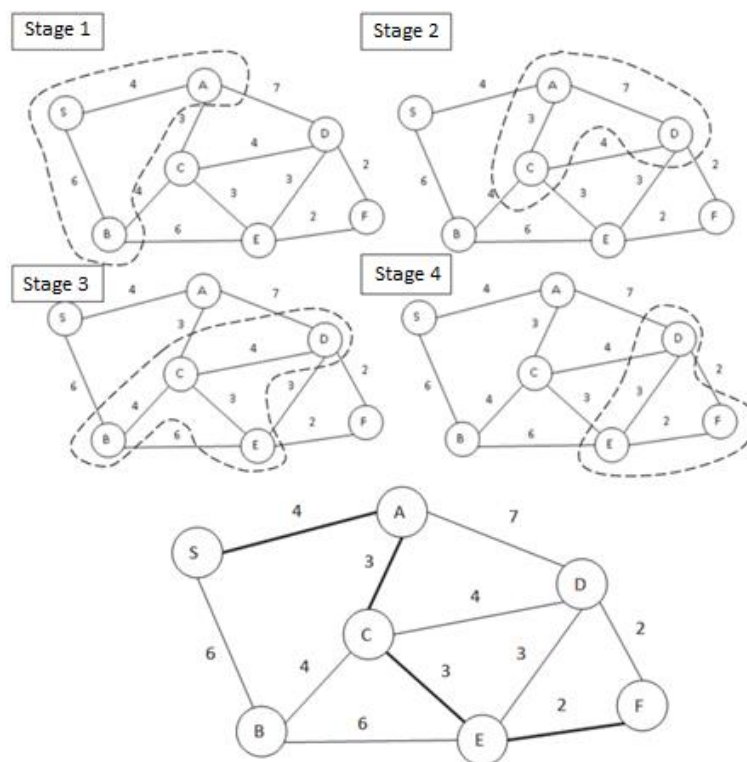


Fig. 1. Dijkstra's algorithm procedure
Source: [1]

The vertex of S is the source node and the vertex F is the ending node. Each edge in the graph is weighted (non-negative). The operation of the Dijkstra algorithm is to find the vertex connected to the source node by the lowest weight common edge, which in the figure is the connection of the source node S to node A. Then the node connected to the source node takes over its role (A). This iteration continues until the endpoint (S-> A-> C-> E-> F) is reached. The figure shows (with

a bold line) the path with the lowest sum of weights ($4 + 3 + 3 + 2 = 12$). Their sum was 12 and represents the optimal route (minimum cost to get there) between nodes S and F.

The Dijkstra algorithm is commonly used in single vehicle routing programs. On the basis of this algorithm works, among others route mapping system in Google Maps.

Marine adaptation of Dijkstra's algorithm

In order to adapt the Dijkstra algorithm for marine navigation, it is necessary to consider the following aspects:

1. Provide a method of weighing sections of the route that are adequate to the specificity of maritime navigation, thus:

a. Take into account that some edges will be faster than others due to the optimal matching of the sailing characteristics of the yacht and the wind that blows in a given geographic square at a given time.

b. Take into account that reaching the boundary of the geographic square requires providing new weather data for the next period of time.

2. Provide a map with areas where it is possible to swim safely without reaching the land / shallow water.

3. Provide a map with areas where it is not safe to swim:

a. sailing is risky (e.g. shallow water, forecasted storm in a given time window)

b. sailing is uncomfortable (high wave, strong swing)

c. sailing is forbidden (fishing grounds, military zones, etc.)

4. Take into account the effect of sea currents coinciding with certain edges of the voyage and adding to the speed of the yacht

5. Take into account the drift of the yacht, so the need to set a different sailing angle to correct the wind and wave drift of the yacht

6. Provide such detailed map squaring that it is possible to precisely avoid small water obstacles - eg objects 100 meters wide.

7. Provide a routing procedure based on an interactive approach - first rough topology of edge points, then correction for detailed map and weather conditions.

The inclusion of some of these guidelines is described in the Implementation section. All of them will be fully implemented in the next development of the algorithm.

Implementation

The solution was implemented as a set of tables and stored procedures of the PostgreSQL database with the PostGIS spatial extension and the PG_Routing routing machine.

For efficiency reasons, the operation of the algorithm has been divided into two phases:

- In the preliminary phase, all global and time-stable data are prepared, performing more time-consuming operations, such as calculating the land content in the mesh, preparing the polar plots of yachts, determining the edges for initial routing or determining the vertices of the topological graph used in later steps to determine the final routes.

- In the proper phase, only the operations necessary to calculate the route are performed and only on the part of the space in which the route will be mapped. This allows for a significant acceleration of the algorithm and does not generate unnecessary operations on parts of the space that will not be visited.

During the server operation, cyclic operations such as downloading weather data and updating them in the database are also performed.

The calculation process consists of two phases: the environment preparation phase and the route calculation phase.

The environment preparation phase

Land tables preparation

Initial table with lands is created from Natural Earth [3] data, which is imported into the database using QGIS [7].

Preparation of a table with excluded areas

Excluded areas are created on the basis of data from the OpenStreetMap project [8] by the community gathered around the OpenSeaMap project [9]. The data extract is downloaded and filtered using the osmosis application, and the resulting file is imported into the database with the osm2pgsql processor. The imported data is rewritten to the tables compliant with the solution scheme.

Preparation of a table with the speed of the yachts in relation to the wind

Polar plot is a chart linking the sailing characteristics of the yacht with the strength and direction of the wind that affects it, allowing you to read what speed the yacht will reach in a given direction and strength of the wind.

An example of a polar plot is presented in Fig. 2.

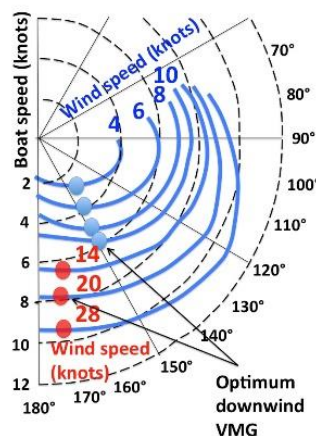


Fig. 1. Polar plot example
Source: [4]

The table with the speed of yachts in relation to the wind is created on the basis of the data available in the repository [5]. As part of the project, a dedicated tool was created that allows you to download this data and import it to the database in a structure consistent with the solution diagram.

Preparation of a table with weather data

For the needs of the solution, a service has been created that periodically downloads current weather data in GRIB format from NOAA GFS [6] sources, extracts the values necessary for the correct operation of the algorithm, and then imports them into the database.

Creation of a table with 0.5 degree squares

Based on the conducted experiments, we determined that the compromised maximum size of a tile is 0.5 degrees (in the future, we will reduce this tile at least 10 times as we increase the processing power). This size is used to create the initial subdivision grid.

Inserting the land fragments intersecting with the square into the table

For each square of the mesh generated in the previous step, a piece of land overlapping with it is separated. The geometry of the land in the later steps is used to determine the land content in the mesh, and when dividing the mesh further, it is used as the land source for the smaller mesh sizes. This approach significantly reduced the time needed to generate the initial data.

Determination of the land content in a square

Based on the comparison of the mesh area of the mesh and the area of the land it contains and the excluded areas, the level of the mesh filling with land is determined in three values:

- f - full - these stitches will be ignored during further processing;
- p - partial - these meshes will still be divided in order to isolate the landless parts from them;
- n - none - these stitches are considered regular and are not further divided.

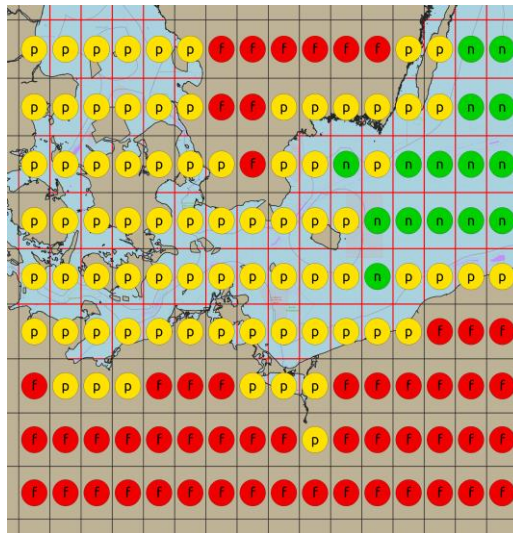


Fig. 2. Identification of tiles with land, with land and water, with only water
Source: own elaboration

Recursive dynamic division of squares with partial land content

The next step is to extract from the meshes, partially land-containing, non-land fragments. Thanks to this, we separate fragments of space through which the yacht can safely move. All the meshes of the semi-land mesh and the exclusion areas are subdivided, the full land meshes are discarded and the landless meshes are left valid. The process takes place in a recursive loop until an

experimentally determined compromise size of the minimum mesh size is reached. This step involves a compromise between the initial resource generation time, the route generation time, and the accuracy of the route and the possibility of determining it in areas densely covered with islands or in narrow straits. In subsequent phases of application development, this tradeoff may be shifted towards accuracy as higher performance is achieved in the routing stage.

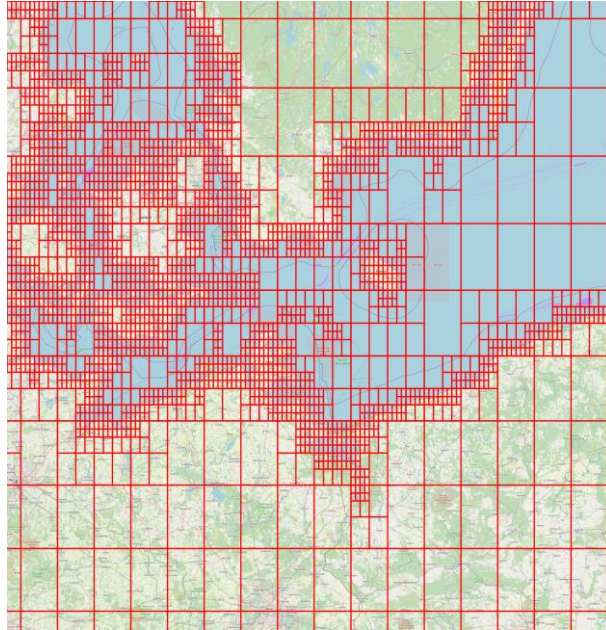


Fig. 3. Recursive separation of squares with land and water into smaller elements
Source: own elaboration

Supplementing the relation to the table with weather data

In the next step, based on the spatial relation, the relation of the foreign key to the table containing weather data is created. The mesh identifier of the weather table is rewritten to all derived elements (edges of the topological graph), which prevents multiple spatial joins and significantly affects the efficiency of the final routing procedure.

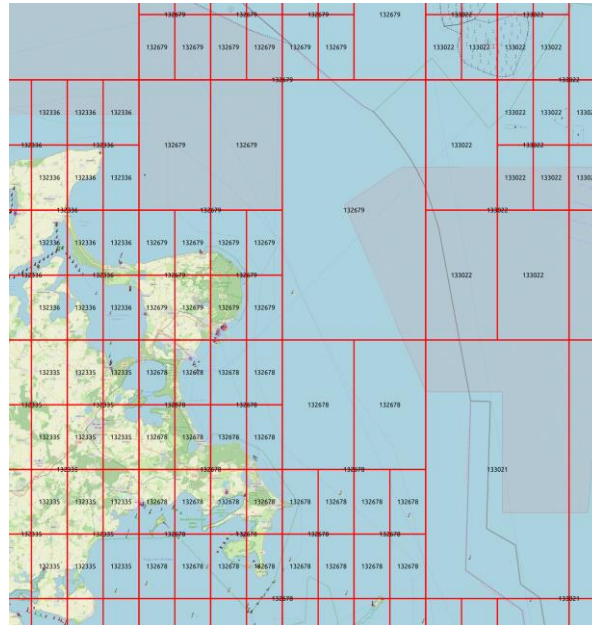


Fig. 4. Adding a link with weather data to the tiles
 Source: own elaboration

Creation of a table with rough edges

In the next step, the topological graph used in the first step of the routing procedure to determine the shortest route, disregarding the weather conditions, is determined between the centroids of the mesh that do not contain land.

Creation of the main mesh

In the next step, on the basis of the coarse mesh, the main mesh is created by dividing the multilines that make up the mesh mesh into individual lines, which in the next steps will be divided and used to create a topological graph used to calculate the target route taking into account weather conditions.

Creation of topology vertices

As the last step of the data preparation phase, points are created on the created mesh, which are used in the next steps of mapping the route as vertices of the topological graph after which the routing will take place. Points are created by dividing each edge of the mesh into 5 parts (experimentally selected parameter).

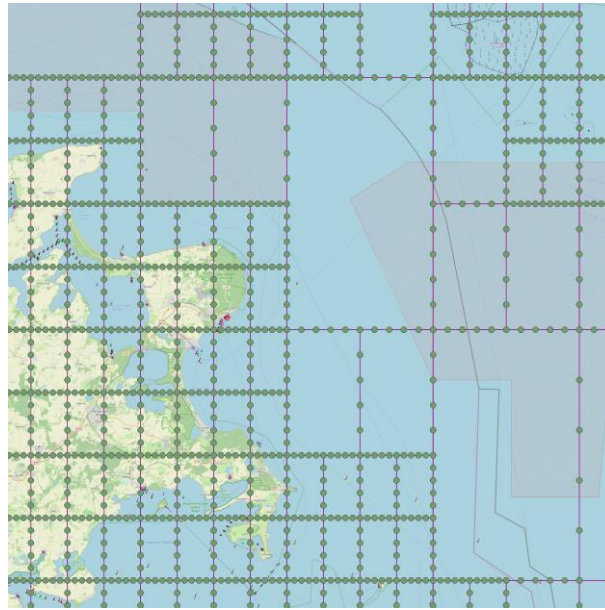


Fig. 5. Topology of the edge points of the tiles
Source: own elaboration

Route calculation phase

Finding the shortest path along a rough topology

The first step in mapping out a route is to find the mesh meshes that intersect with the start and end points, and calculate a rough route. The conducted experiments allowed to determine that the increase in the length of the route due to weather conditions is profitable only in the range of 30%, therefore the final route must directly correspond to the shortest route. Only the edge length was used as the cost of traveling the edge, and the route is determined using a function implementing the Dijkstra algorithm in the PG_Routing extension.

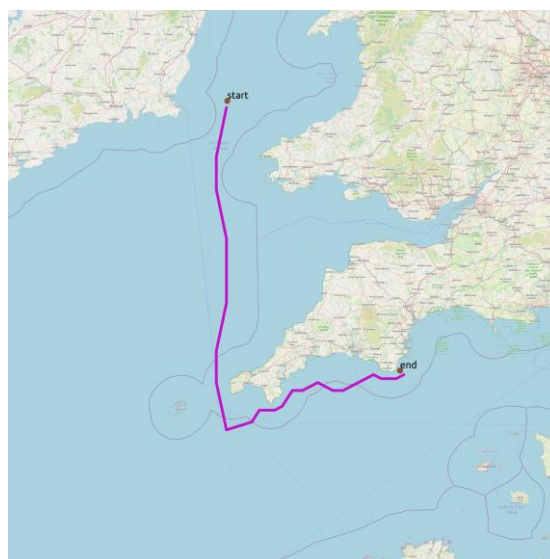


Fig. 6. A simplified route along the rough topology of edge points
Source: own elaboration

Creation a table with edges

At the present stage, we already know which way roughly leads the shortest route between the given points. In the next step, a dense topological graph is determined on the area of the mesh meshes covered by the shortest route, after which we will determine the target route, taking into account weather conditions. The vertices of the topology on the meshes intersecting the coarse route, created during the data preparation phase, are joined by the edges.

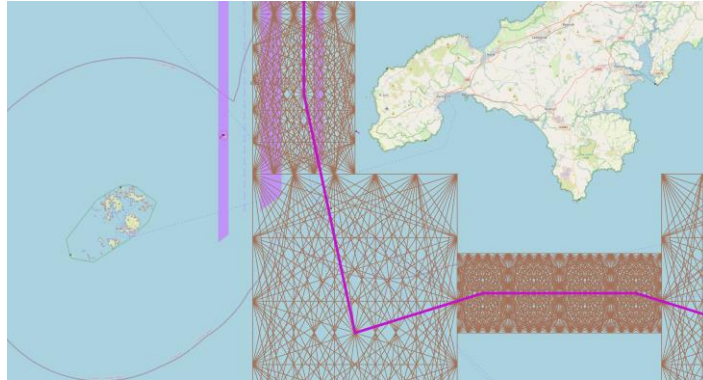


Fig. 7. Detailed topology of marginal points related to the rough route
Source: own elaboration

Attaching the start and end points of the route to the topology

As the previous calculations were made on the basis of the centroids of the mesh meshes traveled, it is necessary to connect the correct start and end points of the route to the topological graph to perform the target route search. For this purpose, the edges of the mesh meshes intersecting with the start and end points are removed, and new edges are created, which start at the route start point and end at the previously prepared topology vertices.

Extending the graph with adjacent tiles

In order to be able to determine the fastest route corresponding to the coarse route, the topology with tiles adjacent must be extended to those on which this route runs. A routine that extends an existing edge set is prepared for recursive operation and can extend the topology multiple times. This point is another compromise point – each expansion of the graph extends the time of calculating the final route, but at the same time increases the probability of finding a much more effective route at a greater distance from the coarse route. In the next steps of the algorithm development, this step can also be made dependent on the calculation result – if the destination route is not found, you can return to it, extend the topology and try to calculate the route again.



Fig. 8. Detailed topology of marginal points related to the rough route
Source: own elaboration

Adding the current and wind information to the edge

The information about currents and winds is added to the designated edges based on the downloaded weather forecasts. The weather information is shifted in time based on the estimated time of reaching each edge. In the next step, the azimuth of each edge and its angles in relation to the wind are calculated both for traveling in and against its direction - these parameters will be necessary to determine the time to pass the edge.

Calculating the time it takes for each edge to travel in both directions

The last operation necessary to prepare the data for the route calculation is the calculation of the time to travel each edge in both directions. Edge crossing times are interpolated on the basis of a table of average yacht speeds for a given yacht type, wind force and direction, which was imported into the system during the data preparation phase.

In Fig. 10 the color of the edge reflects the time in which the edge can be traversed.

At this stage, it is best to notice the differences with the isochronous algorithm popular on the market. The routes determined by the Dijkstra algorithm are located in the tiles associated with the rough route, on the edge points of high density, while in isochronous algorithms these routes are located in funnels generated at a certain angle of inclusion, without being related to geographic tiles and their edge points.

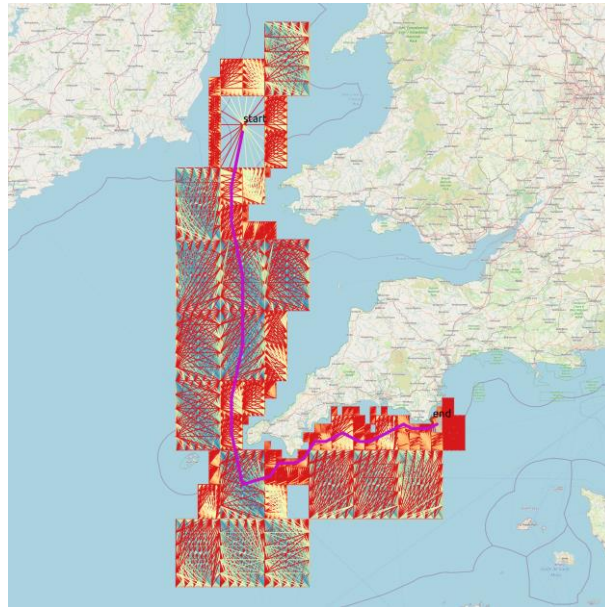


Fig. 9. Generation of different routes and times marked with color
Source: own elaboration

Search for the fastest route along the edges

The data preparation process culminates in mapping the target route on the prepared edges. To calculate the route - as in the case of the coarse route, a procedure implementing the Dijkstra algorithm from the PG_Routing extension is used. In this case, the cost of traversing the edge is the time it takes to travel it, calculated in the previous step.

The Fig. 11 shows the calculated roughing route against the edge with the calculated time of their travel.

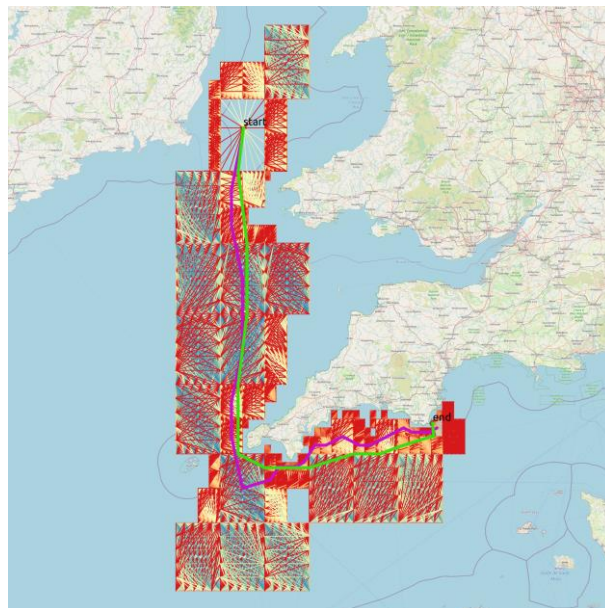


Fig. 10. Determining the optimal route (light green)
Source: own elaboration

The comparison of the coarse route and the destination route against the weather data is as follows.

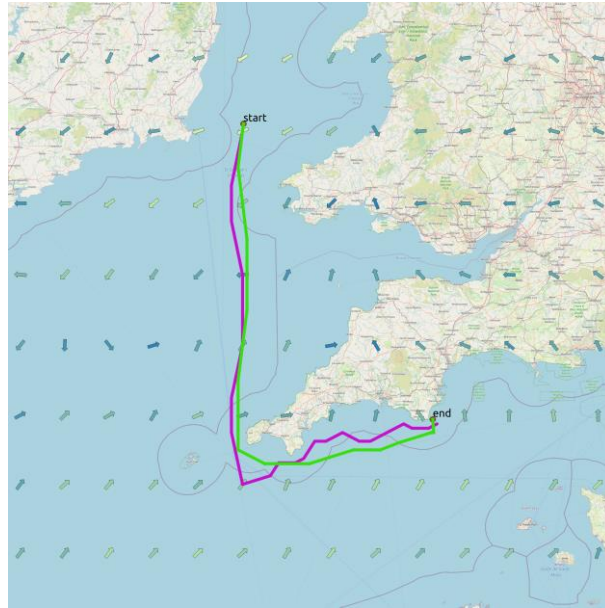


Fig. 11. The coarse route and the optimized route (light green) calculated automatically
Source: own elaboration

Summary

Below are 3 calculations for exemplary routes, for the Salona 44 yacht, for an exemplary weather for a given date.

The "Simplified cruise time" parameter represents approximately the cruise time for a manually marked route, based on manually designated waypoints, converted to the typical speed of a tourist yacht of this class. The parameter "Time of the cruise on the optimized route" shows the effect of the VEO Weather Routing algorithm for map quadratisation of the order of 0.5 degrees (including recursive correction for a given map area). Ultimately, the squaring of maps will reach 0.005 degrees with at least 20 times faster calculations thanks to the use of GPU processors with very high processing parameters. There is further potential to reduce the squares of the map being analyzed and further speed up the algorithms (increasing the computing power of the host computer).

The parameter "Algorithm calculation time in the medium PC class environment" should be treated as a comparative information, giving only an idea of the typical computing load from the perspective of average personal computers.

Tab. 1. Comparison of results gathered with the algorithm usage

Sea route from-to	Cruise time on simplified route (coarse topology)	Cruise time on an optimized route (detailed topology)	Time of calculating the algorithm in the medium PC class environment
Gdynia (marina) - Łeba (port) – ca. 80 mil	16.5h	14.3h	12.8s
Ystad (Sweden) - Roskilde (Denmark) – ca. 150 mil	31.2h	26.1h	15.4s
Krk (town, KRK Island Croatia) - Guajak, Kornat (Croatia) – ca. 80 mil	16.8h	13.4h	12.8s

Source: proprietary calculations

Literature

- [1] Dijkstra E. W., A note on two problems in connexion with graphs, No. 1 (1), pp. 269-271, Numerische mathematik, Jagiellońskiego 2010.
- [2] Tan Y., Wu D., Research on Optimization of Distribution Routes for Fresh Agricultural Products Based on Dijkstra Algorithm, No. 336, pp. 2500-2503, Applied Mechanics and Materials, 2013.
- [3] <https://www.naturalearthdata.com/>
- [4] *Polar diagram*
[https://en.wikipedia.org/wiki/Polar_diagram_\(sailing\)](https://en.wikipedia.org/wiki/Polar_diagram_(sailing))
- [5] <http://jieter.github.io/orc-data/site/>
- [6] <https://www.ncei.noaa.gov/products/weather-climate-models/global-forecast>
- [7] *QGIS system*
<https://www.qgis.org/pl/site/>
- [8] *OpenStreetMaps project*
<https://www.openstreetmap.org/>
- [9] *OpenSeaMaps project*
https://www.openseamap.org/index.php?id=openseamap&no_cache=1

CEMENT MIXTURES FOR 3D PRINTING WITH HIGH ALUMINA CEMENT AS SETTING TIME REGULATOR – EXPERIMENTAL APPROACH

Jakub Uciurkiewicz*, Natalia Gierszewska, Jarosław Błyszko

Department of Reinforced Concrete Structures and Concrete Technology, Faculty of Civil and Environmental Engineering, West Pomeranian University of Technology in Szczecin, al. Piastów 50a, 70-311 Szczecin, Poland

**corresponding author: uciur00@gmail.com*

Abstract:

One of the most important aspects is Set time of concrete. It is very important to print layers one by one without making breaks between. That is why we need to control the open time and set time of printed mixture. This article presents research on combining alumina cement with Portland cement to use with 3D printers. It also shows us how does that mixture reacts when used with Limestone powder, fly ash and superplasticizer. The article discusses the results of tests on different mixtures. Research has shown that thanks to using alumina cement, it is possible to control set time of concrete, depending on the needs.

Keywords:

high alumina cement, 3d printing, cement mixture

Introduction

3D printing methods and usage

Last years have shown us that 3DCP is developing rapidly. It is used more and more, not only in laboratory conditions. One of the greatest advantages of this technique is that it does not need formwork. Concrete 3D printing is used now for a variety of applications, from small objects [e.g. vases] to entire buildings, in future even large-scale buildings [1, 2]. The reason why different methods are used depends mainly on shape, type, and size of the object. Depending on these 3 guidelines, controlling of open time, and set time is very useful. Nowadays it is possible to classify printed objects [3].

Buildability, flowability, extrudability, open time

For 3DCP it is needed to have specific properties of mixture. That is why researchers are looking for different types of cements which will be sustainable for this technology [4]. Buildability is indicator of resistance against failure. It is based on rheological characterization of fresh material used during 3DCP process, and there are ways to improve it in case if it is not good enough [5-8]. Flowability and extrudability are also very important properties of mixture, determined by process of printing. Depending on what type of printer is used, both factors must be customized. Open time is

factor mostly depended on the scale of structure and rate of printing. It is very important to make this time suitable, because of not to spreading the bottom layer when printing other on the top, but also to make them connected at the same time.

Usage of alumina cement with Portland cement

As it is known [A.M. Neville – Properties of Concrete] using Alumina cement with Portland cement when there is from 20% to 80 % of one of the cements might cause instant binding. Thanks to this occurrence it is possible to control set time of mixture of these two cements. Based on this assumption we started testing it in laboratory.

Materials and Methods

Materials

Used Portland Concrete was cement 52.5R Mixed with two types of alumina cements Górkal 40 and Górkal 70, in different mixtures we used additives such as silica fume, fly ash, limestone powder and superplasticizer. We used fine aggregate [0-2 mm]. The compositions are presented in Tab. 1.

Tab. 1 Composition of the mixtures used in the experiment

Concrete	portland cement [g]	alumina cement 40 [g]	alumina cement 70 [g]	fly ash [g]	silica fume [g]	limestone powder [g]	Superplasticizer [g]	Aggregate [g]	Water [g]
C500/40C75	500	75						1500	290
C500/70C75	500		75					1500	290
C500/70C75/FA115	500		75	115			1.2	1500	290
C500/70C75/SF55	500		75		55			1500	290
C500/70C75/SPL1.2	500		75				1.2	1500	290
C125/70C19/LP144	125		19			144		750	145
C125/70C19/LP144/SPL0.6	125		19			144	0.6	750	145
C250/70C38/LP300/SPL0.5	250		38			300	0.5	1500	290

Source: author's own study

Methods

As the measurement methods we used Vicat apparatus to test open time and set time. We also used normalized flow table to check the concrete flow.

Results

Vicat test results

Firstly we made tests on mixtures with 15% of both alumina cements (C500/40C75, C500/70C75). Results are shown in Fig. 1 and Fig. 2, successively for mixture with Górkal 40 and Górkal 70.

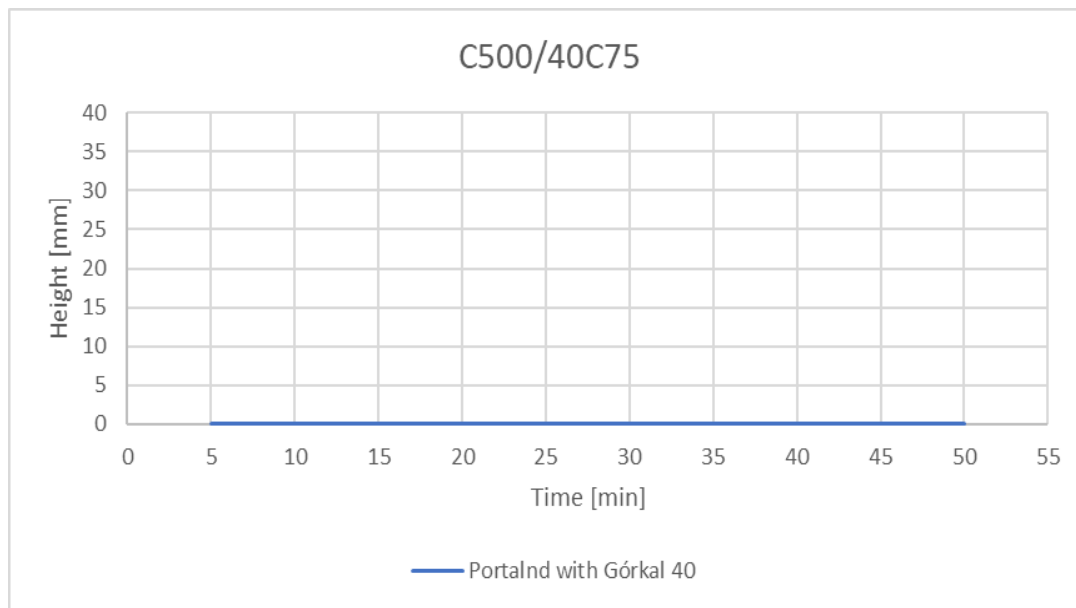


Fig. 1. Vicat measurement results
Source: author's own study

As it is shown in Fig. 2 using mixture of 15% Górkal 70 with portland cement visibly shorten the time of binding of the concrete. However using Górkal 40 did not give us expected effect. After this results we decided to try mixtures with Górkal 70 and additives, and we abandoned further tests with Górkal 40.

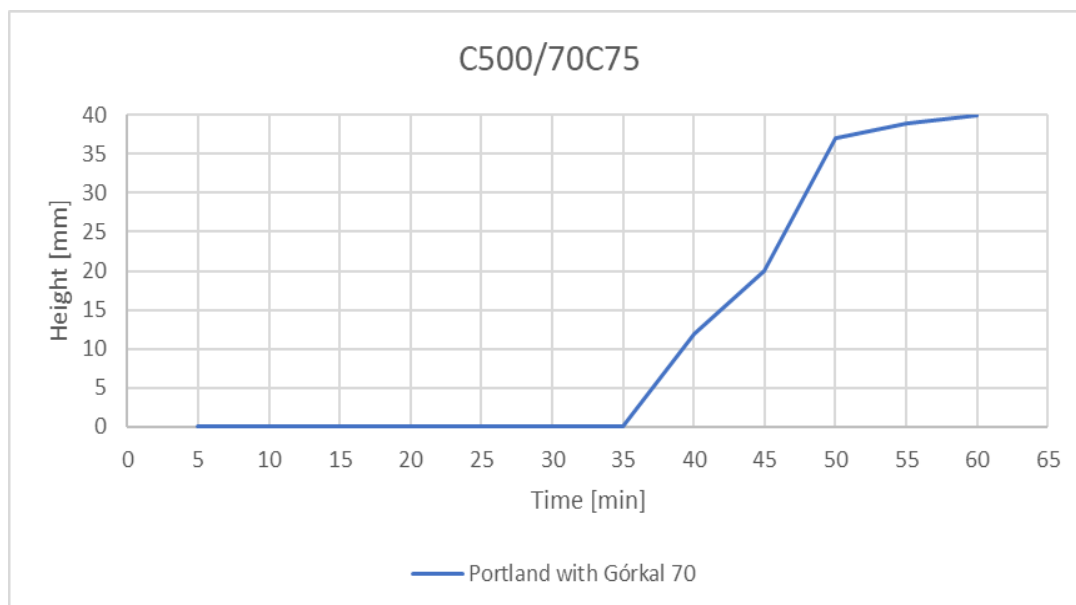


Fig. 2. Vicat measurement results
Source: author's own study

Firstly we added fly ash to our mixture and checked how will it impact on open time of it. Results are shown in Fig. 3.

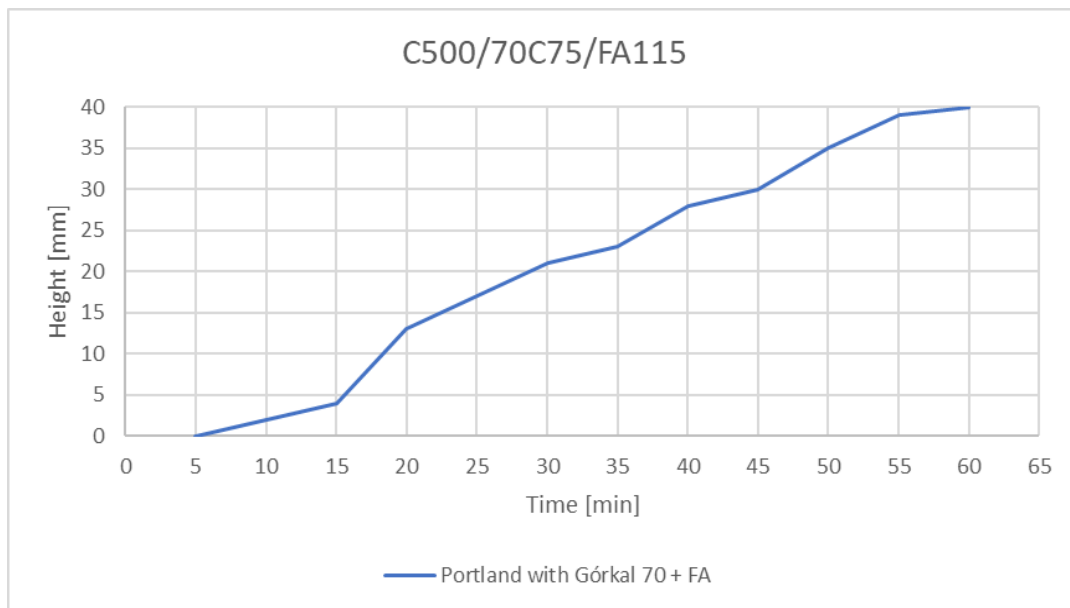


Fig. 3. Vicat measurement results
Source: author's own study

It is clearly visible that adding Fly ash caused some distortion in binding of our mixture, and open time shorten also.

Next we tried adding Silica fume to the same mixture as base in second test. Results are shown in Fig. 4.

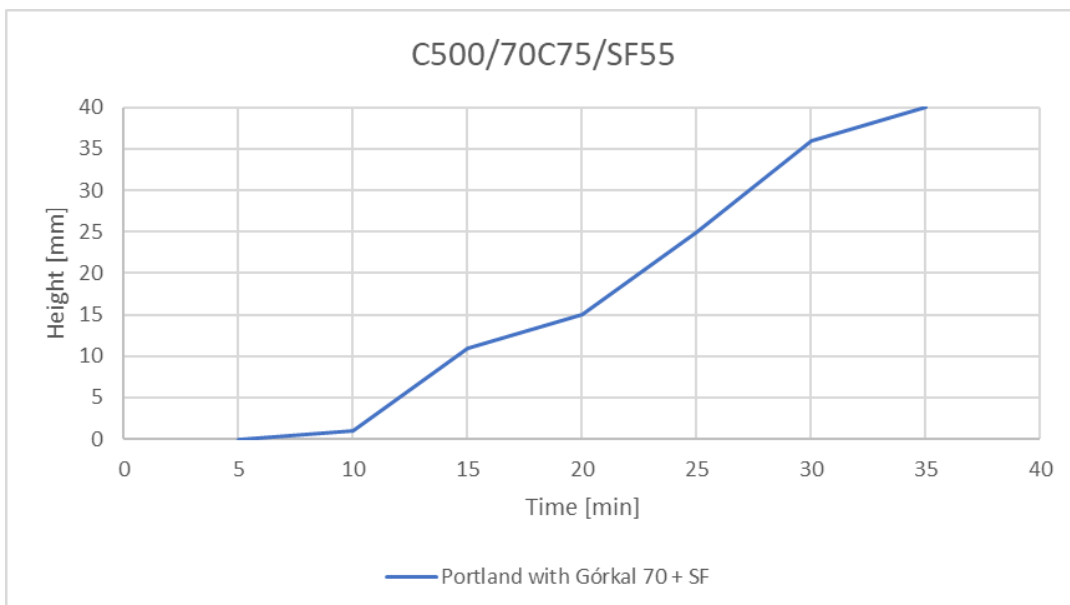


Fig. 4. Vicat measurement results
Source: author's own study

As it is visible, situation at the beginning is similar to the one with Fly ash, but mixture set about 20 minute faster.

Fourth mixture was made with some Superplasticizer. The results are shown in Fig. 5.

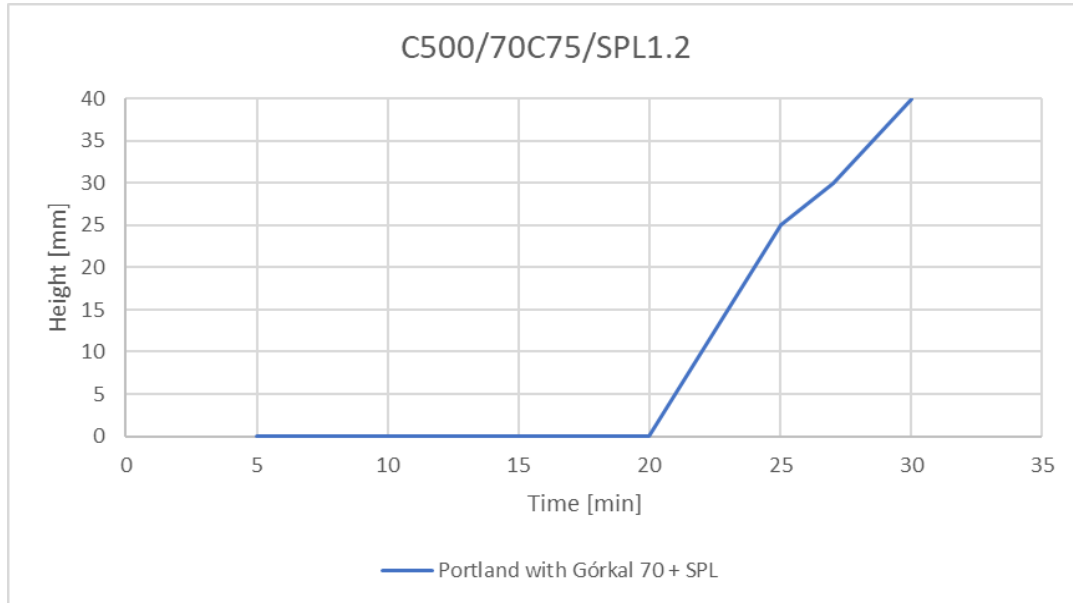


Fig. 5. Vicat measurement results
Source: author's own study

As it is visible, Superplasticizer made the mixture to start bonding 15 minutes faster than the mixture without any additives.

Lastly we decided to check behaviour of the mixture with limestone powder, and limestone powder with superplasticizer. Results are shown in figure 6 and 7 successively for mixture with only limestone powder and then with limestone powder and superplasticizer.

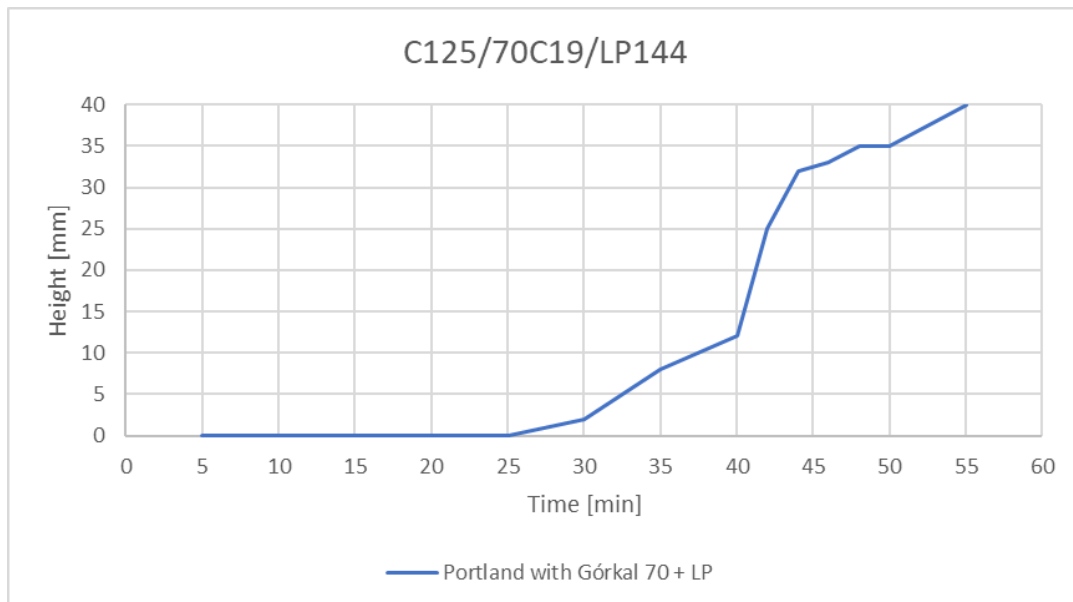


Fig. 6. Vicat measurement results
Source: author's own study

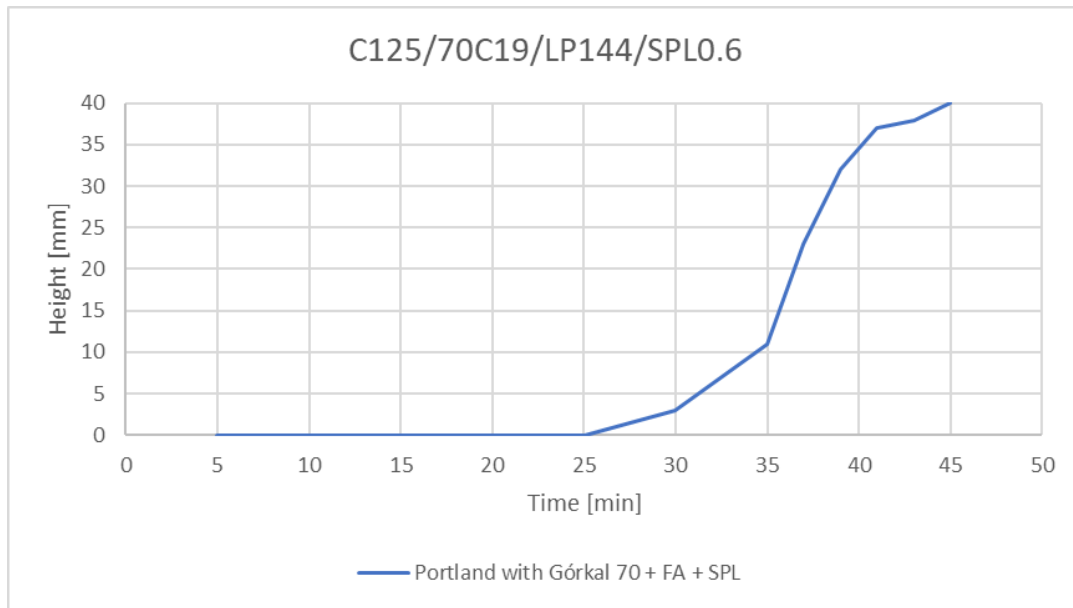


Fig. 7. Vicat measurement results
Source: author's own study

As it is visible, adding Limestone Powder and Superplasticizer gave us results which can be used in further tests.

Slump flow table results

Using the slump flow table was checked the mixture with Limestone Powder and Superplasticizer. Results are shown in the Tab. 2.

Tab. 2. Slump flow test results in time

C250/70C38/LP300/SPL0.5	
Time [min]	Diameter [mm]
6	165
12	133
18	125

Source: author's own study

Discussion

According to the obtained results, it can be seen that some of additives effects on the mixtures more than the others.

Pure mixtures of two of the cements gave us promising result. That was solid foundation for further tests.

Firstly we tried adding Fly ash which caused destabilization in setting time of mixture. The result was that the binding started too quickly. In case of 3DCP it could make a situation in which two layers would not be able to connect with each other. That might be cause of collapsing printed structure. At second approach we used Silica Fume. The beginning was similar to the mixture with Fly ash. However the mixture bonded way faster. Fast bonding is desired in 3D Printing but in this case open time was too short, what makes this mixture useless in 3DCP. Other case was that flowability of

mixture was not quite as expected so another mixture was made using Superplasticizer. This additive shorten the bonding time of mixture, but gave 20 minutes open time what looked promising.

Lastly we decided to add Limestone Powder, which slightly influenced open time of our mixture. It shorten it for just 10 minutes. Still its open time was satisfactory [25 minutes]. Adding Superplasticizer to the last mixture shorten bonding time, but did not affect at open time at all. That result was very promising, because at once we had good flowability of mixture, controlled open time, and fast bonding.

Conclusions

Findings Summary

Based on the test it is possible to use high-alumina cements in 3D printing methods. Especially, that adding specific amount of alumina cement give us possibility to control open time of the mixture. As it is known alumina cements are not cheap for now. But in our method it is used more like additive material than base material. In connection with Limestone Powder, and Superplasticizer it gives the user simple solution. It might be a good alternative for complex Portland cement mixtures with many additives to be used as base material for 3DCP.

Future works

Analysing the results presented in this article it is very promising subject for further tests. In next approaches it will be checked how is the mixture real printability as well as buildability.

Acknowledgements

This research was supported by ZUT Highfliers School (Szkoła Orłów ZUT) project, co-ordinated by Dr. Piotr Sulikowski, within the framework of the program of the Minister of Education and Science [Grant No. MNiSW/2019/391/DIR/KH, POWR.03.01.00-00-P015/18], co-financed by the European Social Fund, the amount of financing PLN 1,704,201,66.

References

- [1] M. T. Souza, I. M. Ferreira, E. G. de Moraes, L. Senff, A. P. Novaes de Oliveira, *3D printed concrete for large-scale buildings: An overview of rheology, printing parameters, chemical admixtures, reinforcements, and economic and environmental prospects*, Journal of Building Engineering, Volume 32, 2020, 101833, ISSN 2352-7102, <https://doi.org/10.1016/j.jobbe.2020.101833>.
- [2] J. Xiao, G. Ji, Y. Zhang, G. Ma, V. Mechtcherine, J. Pan, L. Wang, T. Ding, Z. Duan, S. Du, *Large-scale 3D printing concrete technology: Current status and future opportunities*, Cement and Concrete Composites, Volume 122, 2021, 104115, ISSN 0958-9465, <https://doi.org/10.1016/j.cemconcomp.2021.104115>.
- [3] R. Duballet, O. Baverel, J. Dirrenberger, *Classification of building systems for concrete 3D printing*, Automation in Construction, Volume 83, 2017, Pages 247-258, ISSN 0926-5805, <https://doi.org/10.1016/j.autcon.2017.08.018>.
- [4] S. Bhattacharjee, A. S. Basavaraj, A.V. Rahul, M. Santhanam, R. Gettu, B. Panda, E. Schlangen, Y. Chen, O. Copuroglu, G. Ma, L. Wang, M. A. B. Beigh, V. Mechtcherine,

- Sustainable materials for 3D concrete printing, Cement and Concrete Composites*, Volume 122, 2021, 104156, ISSN 0958-9465, <https://doi.org/10.1016/j.cemconcomp.2021.104156>.
- [5] R. Jayathilakage, P. Rajeev, J.G. Sanjayan, *Yield stress criteria to assess the buildability of 3D concrete printing*, *Construction and Building Materials*, Volume 240, 2020, 117989, ISSN 0950-0618, <https://doi.org/10.1016/j.conbuildmat.2019.117989>.
- [6] F.P. Bos, P.J. Kruger, S.S. Lucas, G.P.A.G. van Zijl, *Juxtaposing fresh material characterisation methods for buildability assessment of 3D printable cementitious mortars*, *Cement and Concrete Composites*, Volume 120, 2021, 104024, ISSN 0958-9465, <https://doi.org/10.1016/j.cemconcomp.2021.104024>.
- [7] J. Kruger, S. Zeranka, G. van Zijl, *3D concrete printing: A lower bound analytical model for buildability performance quantification*, *Automation in Construction*, Volume 106, 2019, 102904, ISSN 0926-5805, <https://doi.org/10.1016/j.autcon.2019.102904>.
- [8] S. Muthukrishnan, S. Ramakrishnan, J. Sanjayan, *Technologies for improving buildability in 3D concrete printing*, *Cement and Concrete Composites*, Volume 122, 2021, 104144, ISSN 0958-9465, <https://doi.org/10.1016/j.cemconcomp.2021.104144>.

APPLICATION OF THE MOLECULAR ELECTRON DENSITY THEORY TO DESCRIBE THE REACTIVITY OF NITRILE N-OXIDES AND SELECTIVITY OF THEIR REACTIONS WITH SELECTED π -DEFICIENT UNSATURATED COMPONENTS

Karolina Zawadzińska*, Karolina Kula

Faculty of Chemical Engineering and Technology, Department of Organic Chemistry and Technology,
Cracow University of Technology, Warszawska 24, 31-155 Cracow, Poland.

*corresponding author: karolina.zawadzinska@doktorant.pk.edu.pl

Abstract:

Molecular Electron Density Theory (MEDT) is a new, powerful tool that could be used to predict the reactivity and mechanism of many organic reactions. In following paper the MEDT was used to describe the nature of addends in [3+2] cycloaddition which provides five membered heterocycled compounds – isoxazoles and their analogs. The most popular group of dipoles in [3+2] cycloaddition – nitrile N-oxide was characterised. Reactivity and behaviour of nitrile N-oxides in the reactions with selected π -deficite components was studied. Following paper provides an overview of the available literature.

Keywords:

nitrile N-oxides, MEDT, DFT, chemical reactivity, computational chemistry

Introduction

Cycloaddition reaction is the most valuable organic proces that is analysed not only from theoretical but also from practical point of view. The general rules of [3+2] cycloaddition was proposed in 1960s. by Huisgen. Since then the prediction of regio and stereochemistry of this reaction has been real challenge [1]. Due to [3+2] cycloaddition it is possible to obtain fivemembered heterocyclic compounds that plays a major role as biologically active agents. Reaction allows obtaining the isoxazoline ring with "full atomic economy" and full usage of substrates [2,3]. Most of the synthesis of isoxazolines in a course of [3+2] cycloaddition go under mild, non-catalyst, condition giving high yields [2,4]. Isoxazoles are used in many important organic transformations, for example in the stereocontrolled synthesis of β -lactam antibiotics, β -amino acids, C-disaccharides, as well as imino or amino polyols [5]. By themselves, these compounds exhibit a variety of biological activities and therefore belong to the wide variety of pharmacophores used in many therapeutic agents. Moreover, they exhibit insecticidal, antibacterial, antibiotic, anticancer, antifungal and anti-tuberculosis properties [6]. Moreover, nucleosides that contain isoxazole moieties exhibit trans-viral

[7], antimicrobial, anti-inflammatory and anti-HIV activity, and some compounds of this group are classified as antidepressants [6, 8].

Nitrile N-oxides – selected aspects of the physicochemistry

Nitrile N-oxides are organic compounds that have in their structure a highly reactive functional segment $\text{C}\equiv\text{N}-\text{O}$, which is why these compounds are considered as a versatile key intermediates in many organic synthesis [9]. Highly polarized bonds C-N and N-O are responsible for those specific properties of nitrile oxides [10]. Majority of nitrile oxides are very reactive but also very unstable, some of them could be explosive. They can undergo rapid dimerisation to furoxans due to the route shown in Fig.1.

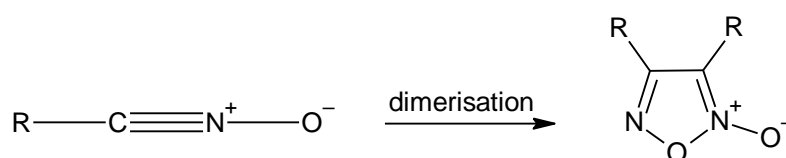


Fig. 1. Dimerisation of nitrile N-oxides

Source: [2]

The dimerisation proceeds at ambient temperature and is much easier in case of aliphatic nitrile oxides [9, 10]. It is found that acetonitrile N-oxide is the most unstable and only after less than 1 minute it dimerizes into furoxane. On the other hand, benzonitrile N-oxides are more stable group, some of them such as para substituted benzonitrile N-oxide could be separated as crystalline products [11, 12]. Stability of nitrile N-oxides correlates with the presence of proper substituent in their structure. For example in aromatic structure, the presence of electron donor or acceptor in the para position can make the compound more stable whilst the electron withdrawing substituents in ortho position do the opposite [13, 14]. What is more, Huisgen, after describing first methodology of [3+2] cycloaddition, proposed the compounds order in which nitrile oxides can be categorized as strong 1,3-dipoles very useful in [3+2] cycloaddition reactions [1].

Among many ways to obtain nitrile N-oxides there will be describe only few in following paper. It is very common to generate nitrile N-oxides in situ due to their issues with instability. There are many methods of generation of nitrile N-oxides. The well known synthesis of both stable and unstable nitrile N-oxides is transformation of aldoximes via halogenation and dehydrohalogenation process. Hydroximoyl halides can be prepared by halogenation of proper aldoximes in the use of N-bromo- and N-chlorosuccinimides or gaseous chloride [11] and in the next step using usually triethylamine or different agent proceed dehydrohalogenation resulting of obtaining nitrile N-oxide [1, 11-15]. Mukayama procedure is the next reaction of generation nitrile N-oxides, especially acetonitrile N-oxide. Mukayama method is based on dehydration of primary nitroalkanes with use of aryl isocyanate in the presence of triethylamine as a base. This method mainly provides unstable nitrile oxides (Fig. 2.) [16]. The dimerization process of nitrile N-oxides can be reversible via for example photolysis or electron impact which also can be considered as a way of generation nitrile N-oxides [17].

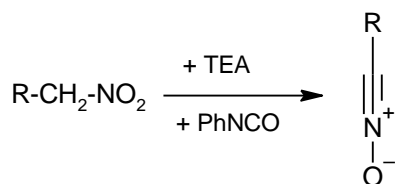


Fig. 2. Synthesis of nitrile N-oxide via Mukayama protocol
 Source: [9]

Due to the aforementioned presence of the $\text{-C}\equiv\text{N-O}$ segment in their structure, nitrile N-oxides are very reactive compound that can be used in many organic synthesis. Without any other compounds they undergo rapid dimerization process or isomerisation to isocyanates. Dimerisation process can be proceed during generation of nitrile N-oxides when there is no other compounds or the reagent is too „weak” to react. Isomerisation process demands thermal or photostimulation. It is known that sterically stabilized nitrile oxides can only undergo isomerisation while heating [18]. The most popular reaction between nitrile N-oxides and different dipolarophiles is [3+2] cycloaddition and it is used as a great way of synthesis of heterocyclic five membered compounds which occur to be biologically active agents [11-16].

Molecular Electron Density Theory

Molecular Electron Density Theory is a new tool for organic reactions to predict the reactivity of components. It is based on the idea that while in the ground state energy the distribution of electron density is responsible for physical-chemical properties of molecule in the ground of DFT rules, here the capability of those changes in electron density describes the molecular reactivity. Using MEDT to describe the [3+2] cycloaddition reactions allows also prediction of mechanism such as pseudoradical, carbenoid and zwitterionic type [19]. In the field of this theory many scientists do their calculations to predict the reactivity in organic reactions. The calculations includes determining such indices as global reactivity indices (electronic chemical potential μ , chemical hardness η , global electrophilicity ω , global nucleophilicity N). They can be estimated according to the equations proposed by Parr[20] and *Domingo* [21-23]. In particular, the electronic chemical potential and chemical hardness of the reactants can be evaluated in terms of the one-electron energies of the frontier molecular orbitals using the following equations [21, 22]:

$$\mu \approx (\text{E}_{\text{HOMO}} + \text{E}_{\text{LUMO}})/2$$

$$\eta \approx \text{E}_{\text{LUMO}} - \text{E}_{\text{HOMO}}$$

Next, the values of μ and η obtained in previous step can be used for the calculation of global electrophilicity (ω) according to the formula [23]:

$$\omega = \mu^2/2\eta$$

The local electrophilicity (ω_k) condensed to atom k , which will be the reacting center, was calculated by projecting the index ω onto any reaction centre k in the molecule by using *Parr* functions P_k^+ [24]:

$$\omega_k = \text{P}_k^+ \cdot \omega$$

In the next, it is possible to calculate global nucleophilicity index (N) from the equation [23]:

$$N = E_{\text{HOMO}} - E_{\text{HOMO}}(\text{tetracyanoethene})$$

where the HOMO energy for tetracyanoethylene (TCE) is taken as a reference. The local nucleophilicity (N_k) condensed to atom k was calculated using global nucleophilicity N and Parr functions P_k^- according to the formula [24]:

$$N_k = P_k^- \cdot N$$

The analysis of the mentioned above indices will be explained in the next chapter of this work.

Reactivity of nitrile N-oxides in the light of computational chemistry

It must be pointed out here that the most efficient and versatile method of synthesis isoxazoles is the one via [3+2] cycloaddition between nitrile N-oxides and proper alkenes. Understanding the molecular mechanism is a very serious matter among theoretical chemists. Some of the cycloaddition were described in the base of computational chemistry. Most of the cycloaddition were carried out with use of benzonitrile N-oxides due to their stability and they react better with most dipolarophiles.

Jasiński et al [4]. studied the reaction mechanism between benzonitrile N-oxides and nitroethene as well as its α monosubstituted analogs. The calculations included global and local electronic properties of components, thermodynamic parameters for reactions, energetic profiles etc. DFT computational results with a conclusion that nitroethene is classified here as a strong electrophile. It was pointed out in this part that introducing of different electron-withdrawing group could enhanced the electrophilicity of the compound. What is very interesting at this point, the benzonitrile N-oxide was found to act as a nucleophilic agent, but there were shown two different cases of a behavior. Change of the substituent to a more electron-donating group causes increasing of electrophilic nature of the component. That is why 4-nitro substituted N-oxide is found to be strong electrophile, even stronger than nitroethenes whilst dimethylamino-substituted N-oxide is moderate electrophile and a strong nucleophile. The local electronic properties have shown that the most nucleophilic reaction center is located in the $-\text{C}\equiv\text{N}-\text{O}$ moiety of benzonitrile N-oxides and the strongest electrophilic center is located on β carbon atom of the nitrovinyl molecular segment. This fact forces the mechanism of the making bonds in the product which concludes that obtaining 4-nitroisoxazoles in this process is more favorable path. Surprisingly it conflicts with the experimental data. It was shown that in this process the most probable path is the one leading to 5-nitro-substituted adduct. Next part of the calculations shown that the described process should be considered as polar and one-step which means no zwitterionic intermediates were found [4].

Different behaviour of benzonitrile N-oxide was shown in the calculations for cycloaddition between different substituted benzonitrile N-oxides with series of para-substituted β -nitrostyrene analogues [25] and β -Phosphorylated nitroethenes (Fig. 3.) [26].

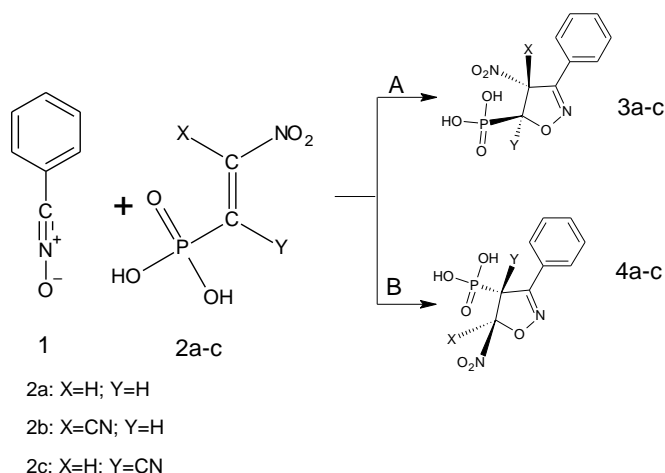


Fig. 3. Theoretically possible paths for [3+2] cycloadditions between benzonitrile N-oxide (1) and β -Phosphorylated nitroethenes
Source: [3]

Global and local electronic properties of benzonitrile N-oxide and both para-substituted β -nitrostyrene analogues [25] and β -Phosphorylated nitroethenes [26] were calculated. The analysis of both cases shown that benzonitrile N-oxide could be classified as moderate electrophile and moderate nucleophile whilst nitroalkenes could play a role of strong electrophiles and marginal nucleophiles. It was found that in those cases more favorable path of the reaction would be the way of forming 4-nitro-substituted isoxazolines which correlates well with calculations. Both processes could be named as one-step and polar reaction. As in previously described work, there can be seen the influence of the presence of strong electron withdrawing group in α -position in nitroalkene on predicted regioselectivity [26].

Domingo et al. [27] have done comparison of two types of nitrile N-oxide in the reaction with alkenes in the field of conceptual DFT study. Studies for the simple nitrile N-oxide which is fulminic acid have shown that this molecule could be classified both as poor electrophile and nucleophile. That means it could participate only in non polar processes with biradical character. The behaviour of fulminic acid was compared to ethylene. On the other hand the benzonitrile N-oxides with a different substituent were studied and considered one show important change in reactivity being classified as good electrophile and nucleophile. The change in reactivity of benzonitrile N-oxides with such alkenes is caused by presence of the phenyl group that cause larger nucleophilic effect. It is expected that benzonitrile N-oxide can take part in polar process. In this work the influence of a different substituent to a phenyl ring in benzonitrile N-oxide was described. Presence of weak electron-releasing ($-\text{CH}_3$) and electron withdrawing ($-\text{CF}_3$) groups causes increasing of nucleophilicity of the compound. Stronger effect was observed by introducing $-\text{NO}_2$ and $-\text{OMe}$ groups as substituents that interact directly with molecular π system of benzonitrile N-oxide [27].

Literature

- [1] R. Huisgen, *Angewandte Chemie*, (1963), Vol. 2(1), 565-598.
- [2] A. Łapczuk-Krygier, A. Kačka-Zych, K. Kula, *Current Chem. Lett.*, (2019), Vol 8, 13-38.

- [3] L. R. Domingo, M. Ríos-Gutiérrez, B. Silvi, P. Pérez, *Eur. J. Org. Chem.*, (2018), 1107-1120.
- [4] R. Jasiński, E. Jasińska, E. Dresler, *J. Mol. Model.*, (2017), Vol. 23(13), 1-44.
- [5] K. Kaur, V. Kumar, A. K. Sharma, G. K. Gupta, *Eur. J. Med. Chem.*, (2014), Vol. 77, 121-133.
- [6] K. A. Kumar, M. Govindaraju, N. Renuka, G. Vasanth Kumar, *J. Chem. Pharm. Res.*, (2015), Vol. 7(3), 250-257.
- [7] Y.-K. Zhang, J. J. Plattner, Y. Zhou, M. Xu, J. Cao, Q. Wu, *Tetrahedron Lett.*, (2014), Vol. 55(11), 1936-1938.
- [8] N. N. Namboothiri, N. Rastogi, *Heterocyclic Chemistry*, (2008), Vol. 12, 1-44.
- [9] K. A. Kumar, P. Jayaroopa, *Int. J. Pharm. Chem. Biol. Sci.*, (2013), Vol. 3, 294-304.
- [10] H. Feuer, *Nitrile Oxides, Nitrones, and Nitronates in Organic Synthesis: Novel Strategies in Synthesis, Second Edition*, Hoboken, New Jersey: John Wiley & Sons, 2008.
- [11] E. Cholewka, *Kinetyka reakcji N-tlenków aromatycznych nitryli z trans-β-nitrostyrenami oraz termoliza otrzymanych diarylonitroizoksazolin*, Kraków: Politechnika Krakowska, 1995.
- [12] P. Beltrame, A. Comotti, C. Veglio, *Chem Commun.*, (1967), Vol. 19, 996-997.
- [13] Dondoni, A. Mangini, S. Ghersetti, *Tetrahedron Lett.*, (1966), Vol. 7(39), 4789-4791.
- [14] D. Kohler, G. R. Barrett, *J. Am. Chem. Soc.*, (1926), Vol. 48, 1773-1777.
- [15] L.K.H. Vinograd, N.N. Suvorov, *Chem. Heterocycl. Compd.*, (1970), Vol. 6, 1403-1405.
- [16] T. Mukaiyama, T. Hoshino, *J. Am. Chem. Soc.*, (1960), Vol. 82(20), 5339-5342.
- [17] U. Schollkopf, P. Tome, *Liebigs Ann.*, (1971), Vol. 753, 135-142.
- [18] E. Chlenov, N.S. Morozova, V. I. Khudak, V. A. Tartakovsky, *Bull. Acad. Sci. USSR, Div. Chem. Sci.*, (1970), Vol. 19, 2492-2494.
- [19] L. R. Domingo, *Molecules*, (2016), Vol. 21(10), 1319.
- [20] R. G. Parr, W. Yang, *Density-functional theory of atoms and molecules.*, Oxford, United Kingdom: Oxford University Press, 1989.
- [21] P. Pérez, L. R. Domingo, A. Aizman, *The electrophilicity index in organic chemistry.*, Amsterdam, Holland: Elsevier, 2007.
- [22] P. Pérez, L. R. Domingo, M. J. Aurell, R. Contreras, *Tetrahedron*, (2003), Vol. 59(13), 3117-3125.
- [23] P. Pérez, L. R. Domingo, M. Duque-Noreña, E. Chamorro, *J. Mol. Struct.* (2009), Vol. 895, 86-91.
- [24] L. R. Domingo, P. Pérez, J.A. Saez, *RSC Adv.*, (2013), Vol. 3, 1486-1494.
- [25] K. Kula, *K. Curr. Chem.Lett.*, (2020), Vol. 10, 9-16.
- [26] K. Zawadzińska, K. Kula, *Organics*, (2021), Vol. 2, 26-37.
- [27] L. R. Domingo, E. Chamorro, P. Pérez, *Eur. J. Org. Chem.*, (2009), Vol. 18, 3036-3044.



PROMOVENDI

Oferujemy:

- skład i łamanie tekstu,
- wydruk książek abstraktów i monografii z numerem ISBN,
- oprawę graficzną wydruków,
- organizację konferencji,
- pomoc w organizacji konferencji,
- obsługę informatyczną i administracyjną konferencji.



www.promovendi.pl



[fundacja.promovendi](https://www.facebook.com/fundacja.promovendi)